




Review

# Liquid Crystal Dimers and Smectic Phases from the Intercalated to the Twist-Bend

Corrie T. Imrie <sup>1,\*</sup> , Rebecca Walker <sup>1</sup> , John M. D. Storey <sup>1</sup>, Ewa Gorecka <sup>2</sup> and Damian Pocięcha <sup>2</sup> 

<sup>1</sup> Department of Chemistry, School of Natural and Computing Sciences, University of Aberdeen, Scotland AB24 3UE, UK

<sup>2</sup> Faculty of Chemistry, University of Warsaw, ul. Zwirki i Wigury 101, 02-089 Warsaw, Poland

\* Correspondence: c.t.imrie@abdn.ac.uk

**Abstract:** In this review we consider the relationships between molecular structure and the tendency of liquid crystal dimers to exhibit smectic phases, and show how our application of these led to the recent discovery of the twist-bend, heliconical smectic phases. Liquid crystal dimers consist of molecules containing two mesogenic groups linked through a flexible spacer, and even- and odd-membered dimers differ in terms of their average molecular shapes. The former tend to be linear whereas the latter are bent, and this difference in shape drives very different smectic behaviour. For symmetric dimers, in which the two mesogenic groups are identical, smectic phase formation may be understood in terms of a microphase separation into distinct sublayers consisting of terminal chains, mesogenic units and spacers, and monolayer smectic phases are observed. By contrast, intercalated smectic phases were discovered for nonsymmetric dimers in which the two mesogenic units differ. In these phases, the ratio of the layer spacing to the molecular length is typically around 0.5 indicating that unlike segments of the molecules overlap. The formation of intercalated phases is driven by a favourable interaction between the different liquid crystal groups. If an odd-membered dimer possesses sufficient molecular curvature, then the twist-bend nematic phase may be seen in which spontaneous chirality is observed for a system consisting of achiral molecules. Combining the empirical relationships developed for smectogenic dimers, and more recently for twist-bend nematogenic dimers, we show how dimers were designed to show the new twist-bend, heliconical smectic phases. These have been designated SmC<sub>TB</sub> phases in which the director is tilted with respect to the layer plane, and the tilt direction describes a helix on passing between layers. We describe three variants of the SmC<sub>TB</sub> phase, and in each the origin of the symmetry breaking is attributed to the anomalously low-bend elastic constant arising from the bent molecular structures.

**Keywords:** liquid crystal dimers; intercalated; interdigitated; twist-bend nematic; twist-bend smectic; chirality; resonant soft X-ray scattering



**Citation:** Imrie, C.T.; Walker, R.; Storey, J.M.D.; Gorecka, E.; Pocięcha, D. Liquid Crystal Dimers and Smectic Phases from the Intercalated to the Twist-Bend. *Crystals* **2022**, *12*, 1245. <https://doi.org/10.3390/cryst12091245>

Academic Editor: Ingo Dierking

Received: 15 August 2022

Accepted: 28 August 2022

Published: 2 September 2022

**Publisher's Note:** MDPI stays neutral with regard to jurisdictional claims in published maps and institutional affiliations.



**Copyright:** © 2022 by the authors. Licensee MDPI, Basel, Switzerland. This article is an open access article distributed under the terms and conditions of the Creative Commons Attribution (CC BY) license (<https://creativecommons.org/licenses/by/4.0/>).

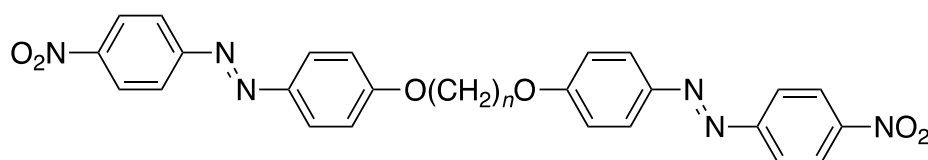
## 1. Overview

Over the last decade arguably the hottest topic in liquid crystals science has been the twist-bend nematic, N<sub>TB</sub>, phase following its discovery in 2011 [1], some ten years after its prediction by Dozov [2]. We will return to the N<sub>TB</sub> phase later, but widely overlooked in Dozov's seminal work was the prediction of twist-bend smectic phases, and in this review, we trace the discovery of these phases for liquid crystal dimers [3]. Although the aim of this Special Issue is to provide an overview of the state-of-the-art of current UK liquid crystals research, the work we describe would not have been possible without a close collaboration between the Universities of Aberdeen and Warsaw. Indeed, the very essence of liquid crystals research is the need for a multidisciplinary approach, and science should know no borders. In keeping with this Special Issue's aim, however, we have attempted to focus primarily on the contribution to the overall work made in Aberdeen, but note that this story is fundamentally one of collaboration.

At the root of this work are liquid crystal dimers, and we begin in Section 2 with a very brief description of the characteristic behaviour of this fascinating class of low molar mass liquid crystals. In Section 3, we consider the smectic behaviour of symmetric dimers, and follow this in Section 4 by describing the discovery of the intercalated smectic phases for nonsymmetric dimers. We then return to describe the  $N_{TB}$  phase in Section 5 and briefly consider the types of liquid crystal dimer known to exhibit the phase. Pulling together the themes developed in Sections 3–5, we describe the discovery of the newest class of smectic phases in liquid crystal dimers, the twist-bend smectic phases in Section 6. We finish this review with an outlook of what may be achieved in this area in the future.

## 2. Liquid Crystal Dimers

Liquid crystal dimers consist of molecules containing two semi-rigid mesogenic moieties linked through a flexible spacer normally, but not always, an alkyl chain, and can be divided broadly into two classes. In symmetric dimers the two mesogenic units are the same, whereas in nonsymmetric dimers they differ. Detailed reviews of structure-property relationships in liquid crystal dimers can be found elsewhere [4–6], whereas for the purpose of this overview we need to consider only what may be referred to as their archetypal behaviour. Figure 1a shows how the melting points and nematic-isotropic transition temperatures,  $T_{NI}$ , vary as the length of the spacer is increased for a series of symmetric liquid crystal dimers, the  $\alpha,\omega$ -bis(4-nitroazobenzene-4'-oxy)alkanes, [7]



and these are referred to using the acronym  $BNABO_n$  in which  $n$  refers to the number of methylene units in the flexible spacer. It can be seen in Figure 1a that  $T_{NI}$  initially exhibits a strong alternation as the parity of the spacer is varied, but that this attenuates on increasing spacer length. In this alternation it is the even members of the series that show the higher values of  $T_{NI}$ . It is interesting to note that the melting points for this particular series also alternate on increasing the spacer length, and again the even members show the higher values, but this is somewhat less regular behaviour than that seen for  $T_{NI}$ , and is not observed for all dimer series. The dependence of  $T_{NI}$  on spacer length and parity in dimers is most often attributed to molecular shape when considering the spacer in its all-*trans* conformation. For an even-membered spacer, the two mesogenic units are more or less parallel, whereas for an odd-membered spacer they are inclined to each other and the molecule is bent (Figure 1b). The linear shape of an even-membered dimer is more compatible with the molecular organisation found in the nematic phase than the bent-shape of an odd-membered dimer, and this accounts for the higher values of  $T_{NI}$  seen for the former. Although intuitively pleasing, this interpretation does not account for the pronounced alternation also observed in the nematic-isotropic entropy change on increasing the spacer length, and to do so the inherent flexibility of the spacer must be accounted for by considering a wide range of conformations and not solely the all-*trans* form [5]. For our purposes, however, it is sufficient to remember that, on average, an even-membered dimer is essentially linear whereas an odd-membered dimer is bent, and that this difference in average shape decreases as the spacer length increases given the increasing number of conformations available to the spacer.

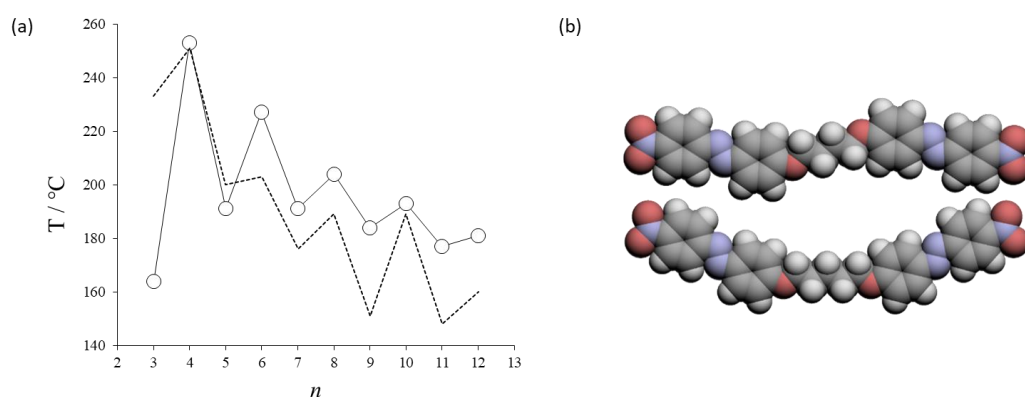
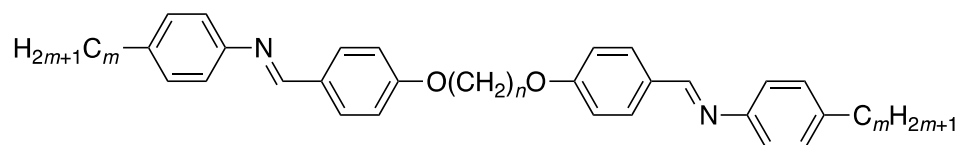


**Figure 1.** (a) The dependence of the nematic-isotropic transition temperatures,  $T_{NI}$ , on the number of methylene groups,  $n$ , in the flexible spacer for the BNABO $n$  series [7]. The circles indicate  $T_{NI}$ , and the broken line joins the melting points. (b) Molecular shapes of BNABO4 (upper) and BNABO5 (lower).

### 3. Symmetric Liquid Crystal Dimers and Smectic Phases

The interest in liquid crystal dimers can be traced back to the early 1980s and the suggestion by Griffin and Britt that they may be used as model compounds for the technologically important semi-flexible main chain liquid crystal polymers [8] whereas their discovery, many decades earlier, by Vörländer had been largely overlooked [9]. The dimeric molecular architecture represented a marked deviation in the design of a low mass liquid crystal. The overwhelming majority of low molar mass liquid crystals up to that point consisted of molecules containing a single semi-rigid core attached to which were one or two flexible alkyl chains. In essence, the interactions between the cores accounted for the liquid crystal behaviour and the terminal chains used to reduce the melting point and drive smectic phases. In a dimer, this structure is inverted and now the core of the molecule is flexible, and we have seen already the importance of this in controlling their shape and hence, transitional behaviour.

The majority of dimers reported in the 1980s showed only nematic behaviour and Griffin and Britt attributed this to their inherent molecular flexibility suppressing smectic phase formation [9]. With hindsight, the absence of smectic behaviour was surprising. It was well-known that molecular inhomogeneity, such as the chemically distinct regions found in a dimer, drives the formation of smectic phases, and there appeared to be no fundamental reason for dimers not to exhibit smectic behaviour. It was almost a decade later, however, before the first family of liquid crystal dimers were reported that showed rich smectic polymorphism, the  $\alpha,\omega$ -bis(4- $n$ -alkylanilinebenzylidene-4'-oxy)alkanes [10]:



and these are referred to using the acronym  $m.O_nO.m$  in which  $n$  and  $m$  refer to the number of carbon atoms in the spacer and terminal chains, respectively. The strategy underpinning the design of this family of dimers was straightforward and centred upon the need to be able to readily vary the lengths of both the spacer and the terminal alkyl chains, a condition met by the  $m.O_nO.m$  molecular architecture. In addition, they may be considered to be the dimeric analogues of the  $N$ -(4- $n$ -alkyloxybenzylidene)-4'- $n$ -alkylanilines known to be a rich source of smectic phases [11].

The versatility in the synthetic approach used to prepare the  $m.O_nO.m$  series allowed for the transitional behaviour of 132 members of the family to be reported [10]. These included varying the spacer length,  $n = 1$ –12, and the terminal alkyl chain lengths,  $m = 0$ –10. These dimers did indeed exhibit rich smectic polymorphism including smectic A and C

phases, hexatic smectic B and F phases, and soft crystal behaviour. Two novel modulated hexatic phases were discovered for the odd-membered dimers having the longest spacers ( $n = 9, 11$ ) and terminal chains ( $m = 10$ ), and in a later study, involving even longer terminal alkyl chains ( $m = 12, 14$ ), further examples were found [12]. In the higher temperature phase, the smectic layers have a periodic modulation analogous to that found in the Sm C  $\sim$  ribbon phase. This modulated hexatic phase is only observed for dimers with an odd parity spacer, suggesting that the average bent molecular shape drives its formation. This is a theme that runs through this overview.

The study of the  $m.O_nO.m$  series revealed that increasing the spacer length for a given terminal chain length promotes nematic behaviour and this is shown for the  $5.O_nO.5$  series in Figure 2. This was surprising and contravened the very general observations at the time that increasing the length of an alkyl chain promoted smectic behaviour in low molar mass mesogens, and that increasing the length of the spacer in a semi-flexible main chain polymer also promoted smectic behaviour. It is also interesting to note that the SmA-I transition temperatures also exhibited a pronounced odd-even effect as the length and parity of the spacer was varied (Figure 2) as seen for  $T_{NI}$  (Figure 1a). This indicates that the bent odd-membered dimers experience greater difficulty in packing into smectic structures than their linear, even-membered counterparts. Increasing the terminal chain length for a given spacer promotes smectic behaviour as seen, for example, for the  $m.O5O.m$  series in Figure 3, and as would be expected.

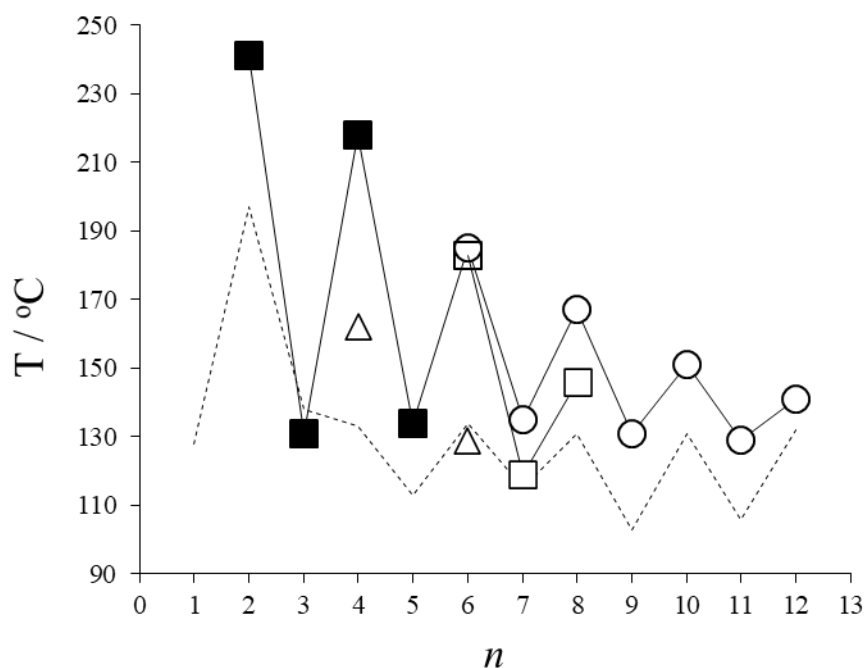


**Figure 2.** The dependence of the transition temperatures on the number of methylene groups,  $n$ , in the flexible spacer for the  $5.O_nO.5$  series [10]. The broken line joins the melting points. Filled squares denote  $T_{SmA-I}$ ; unfilled squares  $T_{SmA-N}$ ; circles  $T_{NI}$ ; triangles  $T_{SmA-SmB}$ .

A simple empirical relationship emerged from the study of the  $m.O_nO.m$  family of compounds relating the observation of smectic behaviour to the relative lengths of the terminal chains,  $m$ , to that of the spacers,  $n$  [10]. Thus, for smectic behaviour to be observed  $m > 0.5 n$ . In addition, all the smectic phases observed for these dimers possessed a monolayer structure, i.e., the layer spacing,  $d$ , corresponded to the full molecular length,  $l$ . These observations are now established as being rather general for symmetric dimers with only a small number of exceptions known [5], and imply that in the smectic layer the mesogenic units, spacers and terminal chains may be considered to microphase separate into distinct sublayers as sketched in Figure 4a. An alternative packing arrangement of the dimers in which the terminal chains and spacers are randomly mixed to give an

intercalated structure (Figure 4b), although entropically favoured, was not observed, and this was attributed to an unfavourable interaction between the terminal chains and spacers offsetting the favourable entropic term [13].

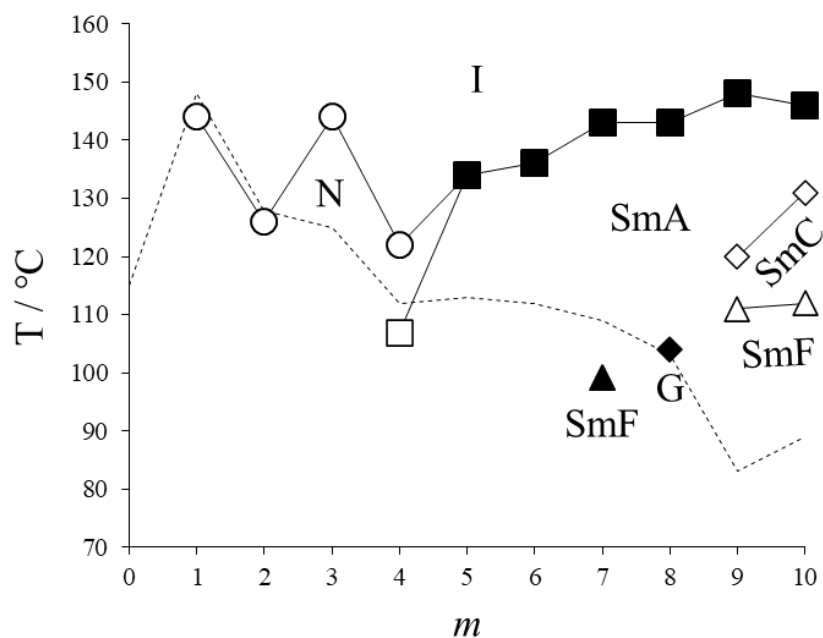


**Figure 3.** The dependence of the transition temperatures on the number of carbon atoms,  $m$ , in the terminal chains for the  $m.O5O.m$  series [10]. The broken line joins the melting points. Filled squares denote  $T_{SmAI}$ ; unfilled squares  $T_{SmAN}$ ; circles  $T_{NI}$ ; unfilled diamonds  $T_{SmASmC}$ ; filled diamonds  $T_{SmAG}$ ; filled triangles  $T_{SmASmF}$ ; unfilled triangles  $T_{SmCSmF}$ .

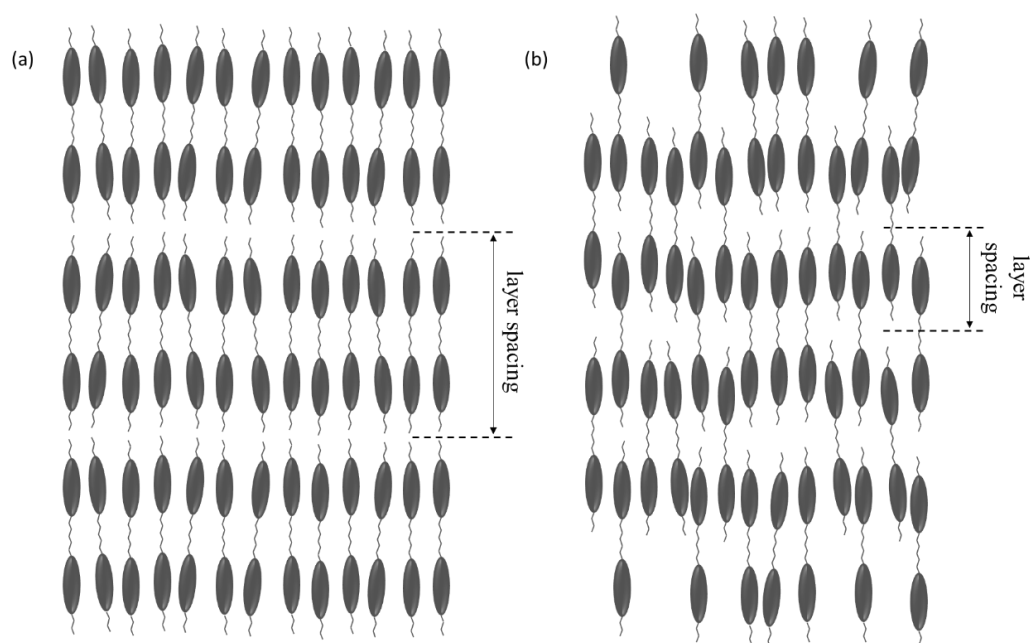
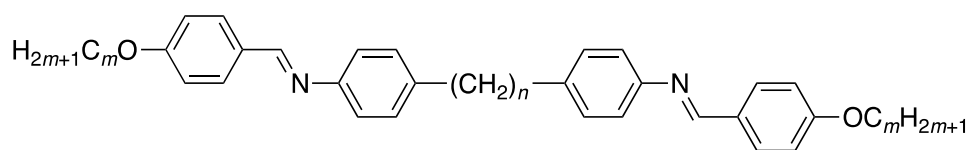


**Figure 4.** A sketch of (a) the monolayer smectic A phase ( $d \sim l$ ) exhibited by symmetric liquid crystal dimers, and (b) the intercalated smectic A phase ( $d \sim l/2$ ) observed only rarely for symmetric liquid crystal dimers.

It is noteworthy that replacing the ether links by methylene links between the spacer and mesogenic units in a dimer has a significant effect on its transitional properties. This is

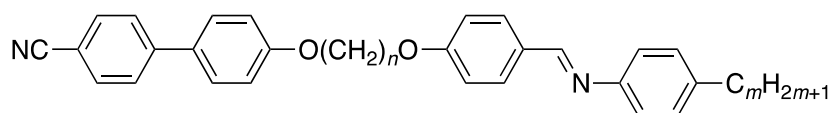
highlighted by a comparison of the behaviour of the  $\alpha,\omega$ -bis(4-*n*-alkoxyanilinebenzylidene-4'-yl)alkanes [14,15],



referred by the acronym *mO-n-Om* in which the hyphen is used to reflect the reversal of the Schiff's base link compared to the *m.OnO.m* series, with that of the corresponding ether-linked materials, the *mO-OnO-Om* series. Surprisingly, for short chain lengths ( $m = 1, 2$ ), the *mO-5-Om* series exhibited a nematic phase and at lower temperatures, a second mesophase that exhibited a fan-like optical texture in coexistence with regions of schlieren texture and this was assigned as an anticlinic, intercalated smectic C phase although its monotropic nature precluded an unambiguous identification using X-ray diffraction (XRD). This behaviour was noted to be in contrast to that seen for the corresponding *mO-OnO-Om* series for which smectic behaviour was observed only if the length of the terminal chains was greater than half that of the spacer, as described earlier for the *m.OnO.m* series. By comparison, the even-membered *mO-n-Om* ( $n = 4, 6$ ) series with short terminal chains showed solely nematic behaviour as expected. For long terminal chain lengths ( $m = 9, 10$ ), the *mO-5-Om* series exhibited a G/J soft crystal phase with a modulated layer structure, whereas the corresponding members of the *mO-6-Om* series a G/J soft crystal phase was observed but with a simple layer structure. This difference in behaviour is similar to that seen for the corresponding members of the *mO-OnO-Om* series. It is important to note that the switch from an ether- to a methylene-linked spacer accentuates the bent shape of an odd-membered dimer as we will see later. The behaviour of the *mO-OnO-Om* series reinforced the view that the difference in shape between odd and even-membered dimers accounts, at least in part, for the differing smectic behaviour observed, with the bent odd-members having a stronger tendency to pack into tilted, alternating lamellar phases. The particularly surprising behaviour seen for *mO-5-Om* with  $m = 1$  and 2, was later shown in fact to be a twist-bend nematic phase and we return to this in Section 5 [16].

#### 4. Nonsymmetric Dimers and Intercalated Smectic Phases

We have seen that symmetric dimers have a strong tendency to form smectic phases having monolayer structures, and that this may reflect an unfavourable interaction between the spacers and terminal chains inhibiting intercalated arrangements. The question now arose: what if we overcame this unfavourable interaction by designing nonsymmetric dimers that exhibited a favourable specific interaction between the unlike mesogenic units, and could this drive the formation of intercalated smectic phases? To investigate this intriguing possibility, the  $\alpha$ -(4-cyanobiphenyl-4'-yloxy)- $\omega$ -(4-*n*-alkylanilinebenzylidene-4'-oxy)alkanes were studied [17,18]:



The acronym used to describe these dimers is *CBO<sub>n</sub>O.<sub>m</sub>*, in which  $n$  and  $m$  refer to the number of carbon atoms in the spacer and terminal chains, respectively. This general structure was chosen because it was known that mixtures of nematogenic 4-*n*-alkoxycyanobiphenyls and *N*-(4-*n*-alkyloxybenzylidene)-4'-*n*-alkylanilines showed induced smectic behaviour implying a specific favourable interaction between the unlike mesogenic units [19,20]. The *CBO<sub>n</sub>O.<sub>m</sub>* family of dimers showed new patterns of liquid crystal behaviour: for example, Figure 5 shows the dependence of the transition temperatures on the length of the terminal chain for the *CBO4O.<sub>m</sub>* series and it is striking that smectic

behaviour is observed for short and long terminal chains, but for intermediate chain lengths only a nematic phase is seen. This behaviour contravened a very general observation for conventional low molar mass mesogens that, for a given series, the smectic A-nematic transition temperature simply increases on increasing the length of a terminal chain and at some point, nematic behaviour is extinguished. To understand the behaviour seen in Figure 5, we must consider how the structure of the smectic phase changes as we increase  $m$ . For short chain lengths, the ratio of the smectic layer spacing to molecular length,  $d/l$  is about 0.5 indicating an intercalated arrangement of the dimers in which differing fragments of the molecules overlap (Figure 6a), the  $\text{SmA}_c$  phase. The driving force for this arrangement was attributed to a specific interaction between the unlike mesogenic units suggested to be an electrostatic quadrupolar interaction between groups having quadrupole moments of opposite signs [21]. We should note that as sketched in Figure 6a the intercalated smectic A phase would appear to be polar, but we assumed that such molecular groupings would be randomly arranged at the macroscopic level such that ferroelectric properties would not be exhibited. This view was later supported by the failure to detect macroscopic polarisation in these phases. Returning to Figure 5,  $d/l$  for the smectic phase shown by the dimers with long terminal chains is around 1.8, implying an interdigitated arrangement of the dimers (Figure 6b), the  $\text{SmA}_d$  phase, and such an arrangement is stabilised by the electrostatic interaction between the polar and polarizable cyanobiphenyl groups while the smectic phase results from the molecular inhomogeneity arising from the long terminal chains. The cross-over from an intercalated to an interdigitated structure arises from insufficient space between the layers of mesogenic units, governed by the length of the spacer, to accommodate the terminal chains and so the layers are pushed apart reducing the specific interaction between the unlike groups. The disappearance of smectic behaviour for intermediate chain lengths reflects a competition between these two incompatible arrangements, neither of which wins and hence, only a nematic phase is observed.

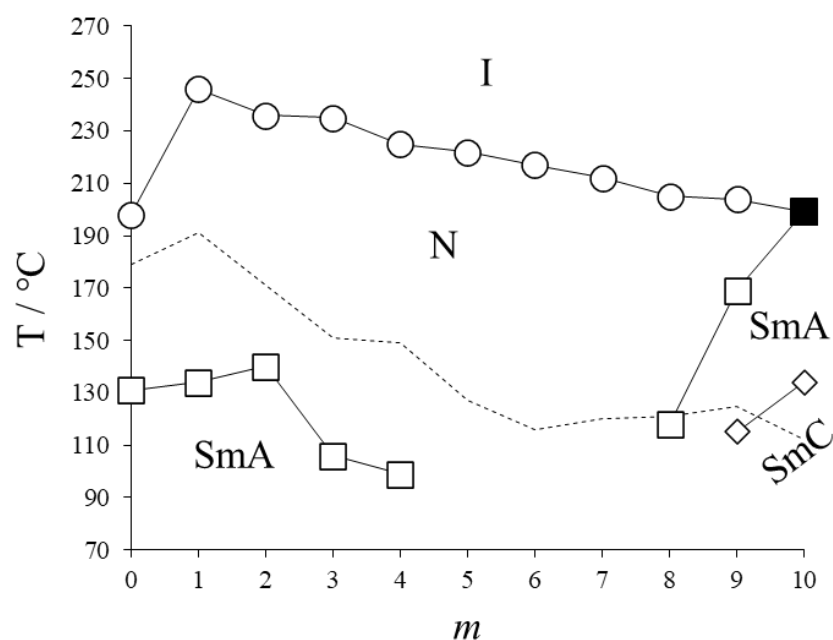


**Figure 5.** The dependence of the transition temperatures on the number of carbon atoms,  $m$ , in the terminal chain for the  $\text{CBO4O.m}$  series [18]. The broken line joins the melting points. Filled squares denote  $T_{\text{SmAI}}$ ; unfilled squares  $T_{\text{SmAN}}$ ; circles  $T_{\text{NI}}$ ; unfilled diamonds  $T_{\text{SmCSmA}}$ .

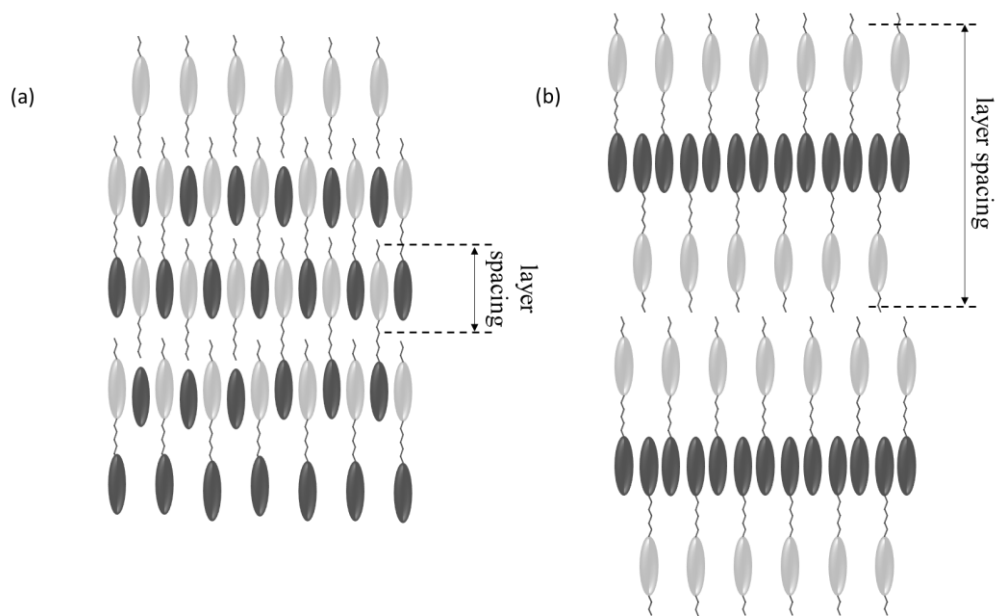


**Figure 6.** Sketches of (a) the intercalated and (b) the interdigitated smectic A phases shown by nonsymmetric liquid crystal dimers.

If we now consider how the phase behaviour changes on varying the length of the spacer while holding the terminal chain constant, Figure 7 shows the behaviour of the CBO $n$ O.10 series [18]. Qualitatively similar behaviour to the CBO4O. $m$  series is seen such that smectic phases are observed for short and long spacers, and exclusively nematic behaviour for intermediate spacer lengths. In contrast to the CBO4O. $m$  series, however, intercalated smectic phases are observed for long spacer lengths and interdigitated phases for short spacers. This is wholly consistent with the view that the terminal chain must be accommodated within the space between the layers that is governed by the length of the spacer.

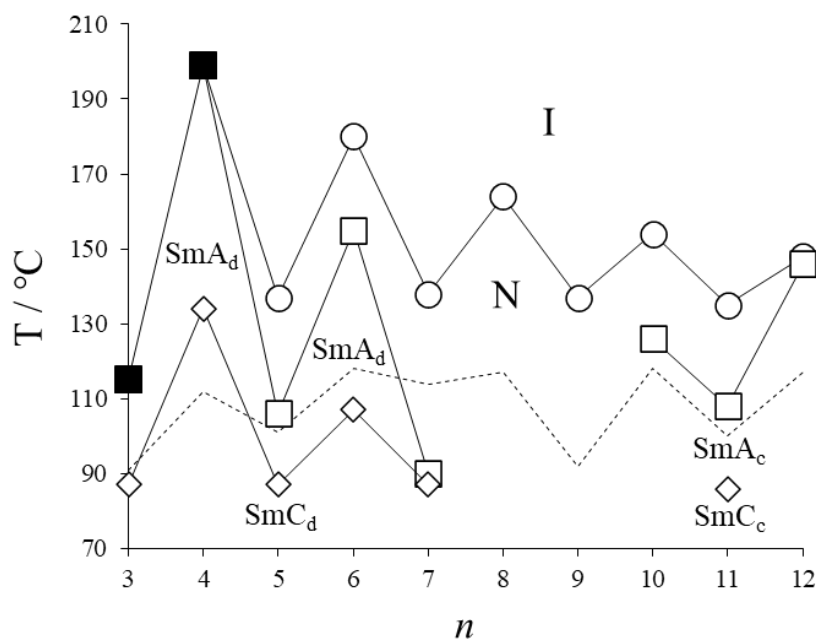


**Figure 7.** The dependence of the transition temperatures on the number of methylene groups,  $n$ , in the flexible spacer for the CBO $n$ O.10 series [18]. The broken line joins the melting points. Filled squares denote  $T_{SmA_I}$ ; unfilled squares  $T_{SmA_N}$ ; circles  $T_{N_I}$ ; unfilled diamonds  $T_{SmCSmA}$ .



Not only was the intercalated smectic A phase shown by the  $\text{CBO}n\text{O}.m$  series but other intercalated variants including the smectic C ( $\text{SmC}_c$ ) and I phases, as well as intercalated soft crystal phases were observed. It is important to note that tilted intercalated smectic phases were observed only for dimers containing long odd-membered spacers, and it was suggested that this reflects the difficulty that these bent dimers experience packing into an intercalated arrangement. Of particular interest was the intercalated smectic C phase shown, for example, by  $\text{CBO}9\text{O}.6$ . The anticlinic structure of the phase was identified on the basis of the observation of a schlieren optical texture containing both  $s = \pm 1/2$  and  $s = \pm 1$  defects [22], and the value of  $d/l$  was established using X-ray diffraction to be about 0.5 indicating an intercalated arrangement of the molecules. A sketch of the molecular arrangement proposed for the intercalated smectic C phase is shown in Figure 8 in which the tilt direction alternates between the layers such that the global tilt angle is zero but locally, within a layer, is non-zero. This structure was later confirmed using electron spin resonance spectroscopy that revealed within the intercalated smectic C phase two distinct directors with azimuthal tilt directions differing by  $180^\circ$  [23]. Within a layer the tilt angle was estimated to be about  $18^\circ$ , fully consistent with the bent geometry of these odd-membered dimers in which the mesogenic units make an angle of around  $15^\circ$  with the spacer. The intercalation of the dimers has been widely accepted to account for the measured values of  $d/l$  of around 0.5 although a number of issues remain to be fully resolved as recently discussed elsewhere [24].

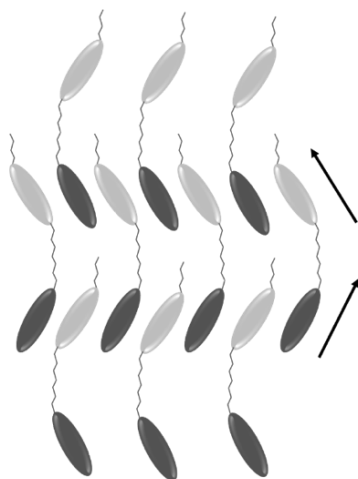


**Figure 8.** Sketch of the molecular arrangement in the intercalated smectic C phase. The arrow indicates the local tilt direction.

In Figure 5, we saw how the transition temperatures varied on increasing the terminal chain length for the  $\text{CBO}4\text{O}.m$  series and this surprising pattern of behaviour was understood in terms of the formation of intercalated smectic phases for short terminal lengths and interdigitated smectic phases for long terminal chains. The behaviour of the  $\text{CBO}5\text{O}.m$  series was very different; see Figure 9. On cooling the nematic phase shown by the members with  $m = 1-9$ , what appeared to be a smectic phase formed, and the values of the transition temperature between this phase and the nematic phase decreased essentially linearly on increasing  $m$ . The structure of the lower temperature phase could not be established using X-ray diffraction due to its monotropic nature. The behaviour seen in Figure 9 was noted as being unusual and it was also noted that the  $\text{CBO}3\text{O}.m$  series showed broadly similar behaviour. These observations were thought to reflect the bent shape of these dimers, but its physical significance was not apparent. As we will see in the next section, however, the behaviour may now be accounted for in terms of the twist-bend nematic phase. Smectic behaviour was observed for long homologues in both these odd-membered series and we will return to this later.

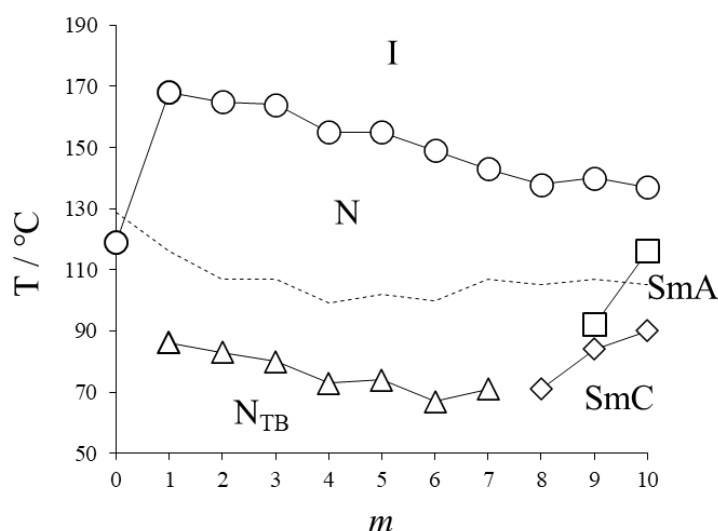
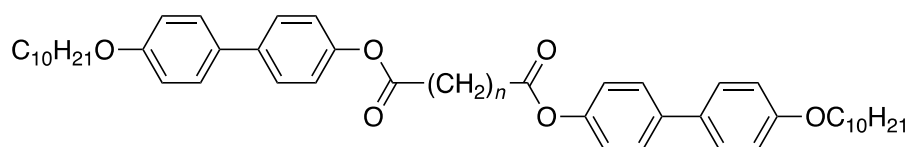


**Figure 9.** The dependence of the transition temperatures on the number of carbon atoms,  $m$ , in the terminal chain for the CBO5O. $m$  series [18]. The broken line joins the melting points. Circles denote  $T_{NI}$ ; triangles  $T_{NTBN}$ ; squares  $T_{SmA}$ ; diamonds  $T_{SmC}$ .

The intercalated smectic phases were first observed for nonsymmetric dimers and as noted earlier, the driving force for their formation was attributed to a specific favourable interaction between the unlike mesogenic units. It was known, however, that a small number of symmetric liquid crystal dimers also showed intercalated smectic phases (see, for example, [25]) although always for long odd-membered spacers. This supported the suggestion that molecular shape was an important factor in smectic phase formation. This tendency for bent odd-membered dimers to pack into tilted, intercalated smectic phases to alleviate the difficulties in packing into orthogonal arrangements has similarities to the behaviour of bent-core mesogens [26]. This view was further reinforced by the behaviour of a series of 4-decyloxy-4'-hydroxybiphenyl esters of  $\alpha,\omega$ -alkanedicarboxylic acids reported by Białecka-Florjańczyk et al. [27]:



The even members of this series showed a tilted soft crystal phase, possibly a G/J phase, whereas the odd members exhibited the B4 phase previously only observed for bent-core mesogenic materials. The B4 phase is thought to consist of bundles of twisted, rope-like smectic ribbons of finite thickness which pack to give macroscopic left- and right-handed domains [28]. The formation of helical nanofilaments in these structures is thought to be driven by the instability of the flat layers arising from the mismatch in the projections of the two crystal lattices associated with each arm of the bent core [29]. The elastic strain required to connect the two lattices may be relieved, at least in part, by bending the layers with saddle-splay curvatures. A similar model is clearly applicable to bent odd-membered dimers although would necessarily have to also include the inherent flexibility associated with the spacer. The observation of such behaviour for this particular series may be attributed to the strong lateral interactions known to exist between biphenyl fragments, a view supported by the observation of the soft crystal phase for the even members. Again, we see that molecular shape is a key factor in the pronounced differences in behaviour between odd and even-membered dimers, and the similarities between bent odd-membered dimers and the semi-rigid bent-core mesogens will be further discussed later.

## 5. The Twist Bend Nematic Phase

We now return to the prediction of the twist-bend nematic,  $N_{TB}$ , phase by Dozov [2] and its subsequent discovery by Cestari et al. [1]. At the root of Dozov's prediction was the assertion that bent molecules have a natural disposition to pack into bent structures, but that pure bend cannot fill space and so is forbidden. Instead, bend must be accompanied by other deformations of the director; either twist or splay. In the case of twist, this gives rise to the twist-bend nematic phase in which the director adopts a helical structure in which it is tilted with respect to the helical axis (Figure 10). Perhaps the most intriguing aspect of Dozov's work was the prediction of spontaneous chirality in a fluid system composed of achiral molecules having no positional order. The helices formed may be either left- or right-handed and equal amounts of both are expected.

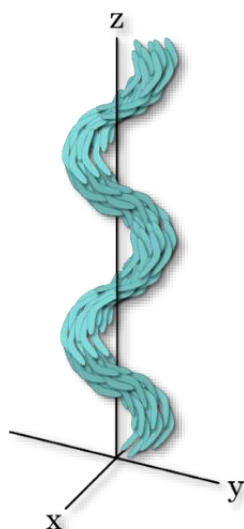
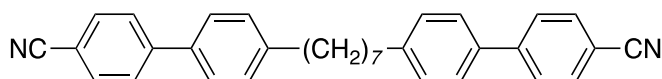


Figure 10. A schematic representation of the twist-bend nematic,  $N_{TB}$ , phase.

Odd-membered liquid crystal dimers with their bent molecular structures (Figure 1b) provided the ideal testbed for Dozov's prediction, and some ten years later, Cestari et al. reported the discovery of the  $N_{TB}$  phase in 1,7-bis(4-cyanobiphenyl-4'-yl)heptane (CB7CB) [1]:



The assignment of the  $N_{TB}$  phase was confirmed using techniques including freeze fracture transmission electron microscopy [30] and resonant soft X-ray scattering (RSOXS) [31]. The events surrounding this discovery are reviewed by Dunmur in another contribution to this collection of papers [32]. A striking feature of the  $N_{TB}$  phase is that the helical pitch is very short, typically around 10 nm, corresponding to around 3–4 molecular lengths. Nematic-nematic transitions had been reported previously for other odd-membered dimers that, with the benefit of hindsight, are examples of  $N_{TB}$ -N transitions [33,34]. A common feature of these dimers is the use of methylene links to connect the spacer to the semi-rigid mesogenic units. By contrast, the majority of dimers reported prior to the discovery of the  $N_{TB}$  phase contained ether-linked spacers, i.e.,  $O(CH_2)_nO$ , although interest in methylene-linked dimers had been triggered earlier by a prediction made by Ferrarini et al. [35,36] that systems containing a high concentration of bent conformers in the isotropic phase should exhibit a nematic-nematic transition. Again, short odd-membered methylene-linked dimers provided a testbed for these predictions. It was found that switching  $O(CH_2)_nO$  for  $(CH_2)_{n+2}$  saw the values of  $T_{NI}$  fall for both odd- and even-membered spacers but the reduction was greater for odd-membered spacers. This resulted in a more pronounced alternation in  $T_{NI}$  for the methylene-linked dimers on varying the spacer length and parity compared

to that seen for their ether-linked counterparts [14,15]. By contrast, the entropy change associated with the nematic-isotropic transition increased for even-membered spacers but decreased for odd-membered spacers on replacing  $O(CH_2)_nO$  with  $(CH_2)_{n+2}$ . These experimental observations were in complete agreement with the predictions of a model described by Luckhurst and co-workers in which the only difference between the dimers is the bond angle between the *para*-axis of the mesogenic unit and the first bond in the spacer [37,38]. For an ether-linked dimer this angle is about  $126.4^\circ$  whereas for a methylene-linked dimer it is around  $113.5^\circ$ . The change in this angle means that an odd-membered methylene-linked dimer is more bent than the corresponding ether-linked dimer (Figure 11). The discovery of the  $N_{TB}$  phase reignited interest in the methylene-linked dimers and previously reported dimers were shown to exhibit the new phase [16]. In addition, odd-membered ether-linked dimers were also shown to exhibit the  $N_{TB}$  phase [39] and led to the reassignment of smectic phases as  $N_{TB}$  phases as shown, for example, in Figure 9 for the CBO5O.*m* series [18,40].

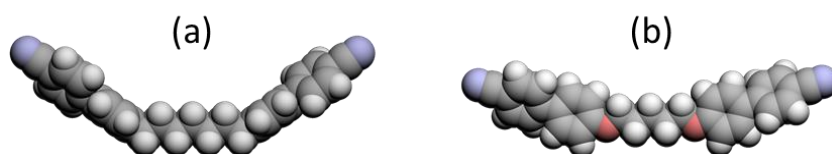
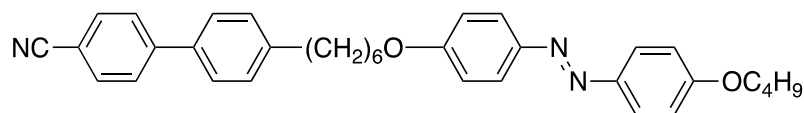


**Figure 11.** A comparison of the shapes of odd-membered methylene- and ether-linked dimers: (a) CB7CB and (b) CBO5OCB.

There is now a large collection of odd-membered dimers known to exhibit the  $N_{TB}$  phase, and structure-property studies have focussed on the nature of the link between the spacer and mesogenic units [41–49], the length and parity of the spacer [39,50–53], the structure of the mesogenic units [54–64], and the chemical nature of the terminal groups [65–68]. Although the majority of twist-bend nematogens are odd-membered dimers, other examples include trimers and higher oligomers [69–74], hydrogen-bonded supramolecular systems [75–79], rigid-bent core systems [80,81] and polymers [82]. A recent overview of structure-property relationships in twist-bend nematogens may be found elsewhere [83].

The overarching structural requirement for the observation of the twist-bend nematic phase is molecular curvature. This is in complete agreement not only with Dozov's model [2], but also with Maier-Saupe theory for V-shaped molecules that predicts the  $N_{TB}$  phase will be formed by just a narrow range of molecular curvatures with the  $N$ - $N_{TB}$  transition temperature being particularly sensitive to the molecular bend angle [84]. The uniformity of molecular curvature is also critical in driving the formation of the  $N_{TB}$  phase as revealed by the behaviour of the azobenzene-based dimer, CB6OABOBu [85]:



This dimer shows an isothermal  $N_{TB}$ - $N$  transition when illuminated using UV-light and this may be attributed to the *trans-cis* photoisomerization of the azo-linkage. This transition is reversible on removing the light source, driven by the thermal *cis-trans* relaxation. The *cis* isomer is more strongly bent than the *trans* isomer (Figure 12) and a priori it may have been expected that increasing the concentration of the more bent isomer would enhance the stability of the  $N_{TB}$  phase. It is clear from this and other studies [86,87] that quite the opposite is true. This counter-intuitive observation was accounted for in terms of the shapes of the two isomers. The molecular curvature of the *trans* isomer is governed by the geometry of the spacer and hence, is spatially uniform. In contrast, the *cis* isomer contains two centres of bend, namely the spacer and the azobenzene fragment, which results in a change in bend polarity along the molecule. This spatially varying bend is not compatible with the local structure of the  $N_{TB}$  phase.

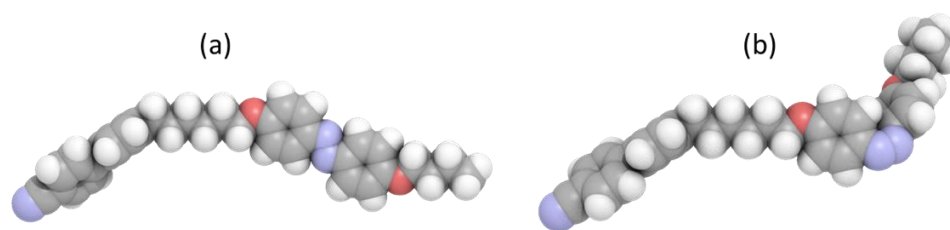
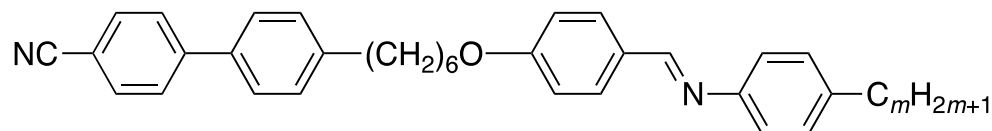


Figure 12. The shapes of the (a) *trans* and (b) *cis* isomers of CB6OABOBu.

## 6. The Twist-Bend Smectic Phases

Dozov, in his seminal work, not only predicted the existence of the  $N_{TB}$  phase for bent mesogens, but also noted that the same arguments could *give rise to a similar symmetry breaking even in apolar banana smectics* [2]. This aspect of the study was largely overlooked, and the search for these twist-bend smectic phases became a focus of our work. At the outset of our studies, the great majority of the  $N_{TB}$  phases reported either vitrified or crystallised on cooling, and only rarely had smectic- $N_{TB}$  or B- $N_{TB}$  transitions been reported [58,88–90]. In designing materials to potentially exhibit twist-bend smectic phases we identified three key structural criteria: (i) a uniform molecular curvature compatible with the  $N_{TB}$  phase, and, based on our previous studies of dimeric smectogens, (ii) a specific favourable interaction between the mesogenic units to promote smectic behaviour, and (iii) a terminal chain that could be readily varied in length to control the packing of the molecules and to promote molecular inhomogeneity.

The first question to address is how does the more pronounced molecular curvature, required to promote the formation of twist-bend phases, affect the tendency of dimers to exhibit smectic phases? Figure 13 shows the dependence of the transition temperatures on the length of the terminal chain for the CB6O.*m* series [40,91]:



in which the hexyloxy spacer ensured the necessary molecular curvature for the  $N_{TB}$  phase to be observed [42]. Our initial study of this series included varying the terminal chain length, *m*, from *m* = 1–10, [40] and in a subsequent study we reported the transitional behaviour of the longer members with *m* = 11–18 [91]. The phase behaviour of the CB6O.*m* series with *m* = 1–10 [40] may be compared to that of the CBO5O.*m* series shown in Figure 9 [18]. The bent nature of both series reduces their smectic tendencies compared to, for example, the linear CBO4O.*m* series shown in Figure 5 [18]. For the CBO5O.*m* series,  $N_{TB}$  phases are observed for *m* = 1–7.  $N_{TB}$  behaviour is extinguished at *m* = 8 and smectic-nematic transitions are observed for *m* = 8–10. For the more bent CB6O.*m* series,  $N_{TB}$  phases are observed for *m* = 1–10, and smectic behaviour emerges at *m* = 10 which exhibits a Sm- $N_{TB}$  transition to be discussed later [40]. This reduction in the smectic tendencies on increasing molecular bend may be quantified by comparing the scaled transition temperature,  $T_{SmN}/T_{NI}$ , for CBO5O.10 of 0.924, with  $T_{SmNTB}/T_{NI}$  for CB6O.10 of 0.909. It is interesting to note that the value of  $T_{NTBN}/T_{NI}$  for CB6O.10 is 0.925, i.e., essentially the same as  $T_{SmN}/T_{NI}$  for CBO5O.10. It appears, therefore, that increasing molecular curvature increases the tendency to exhibit the  $N_{TB}$  phase at the expense of smectic behaviour. Ironically, Dozov highlighted the challenge in obtaining the  $N_{TB}$  phase would be to suppress the formation of smectic phases in bent-core systems [2] in which symmetry breaking had been attributed to specific polar interactions [92]. For odd-membered dimers the origin of the symmetry breaking is quite different and may be attributed to anomalously low values of the bend elastic constant arising from the bent molecular geometry. Thus, the inherent flexibility and bent shape of these odd-membered dimers suppresses smectic behaviour,

and the challenge was to design odd-membered dimers in which the tendency to form smectic phases, rather than the  $N_{TB}$  phase, was enhanced.

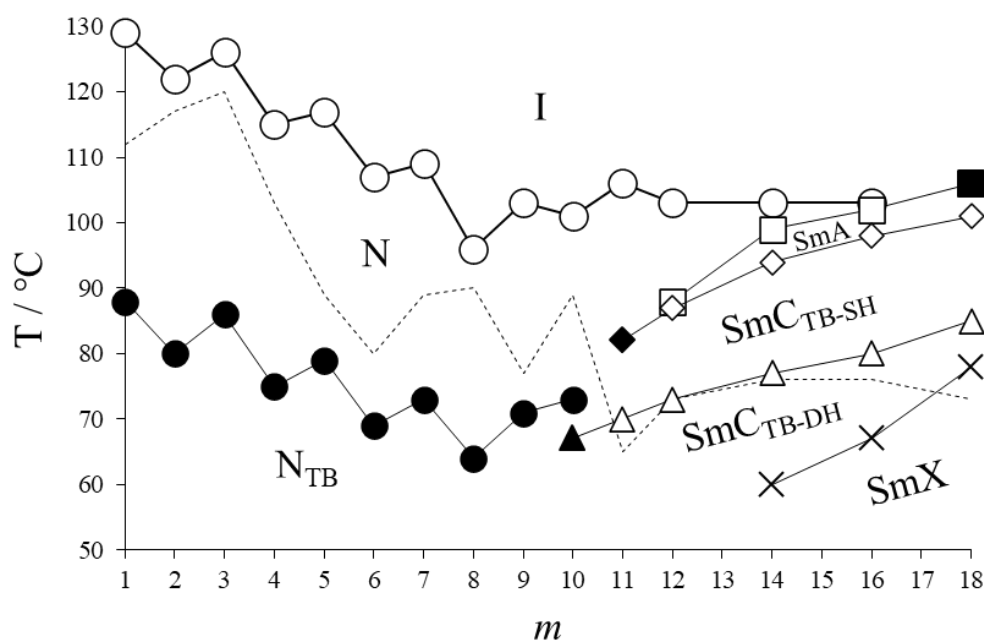
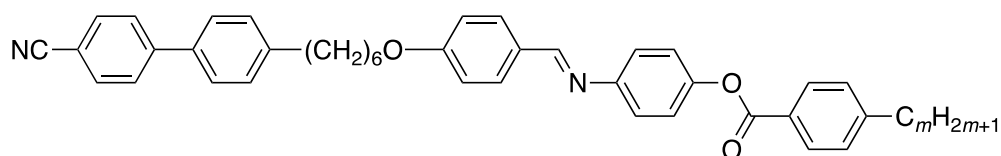


**Figure 13.** The dependence of the transition temperatures on the number of carbon atoms,  $m$ , in the terminal chain for the  $CB6O.m$  series [40,91]. The melting points are connected by the broken lines. Unfilled circles denote  $T_{NI}$ ; filled circles  $T_{NTBN}$ ; filled squares  $T_{SmAI}$ ; unfilled squares  $T_{SmAN}$ ; unfilled diamonds  $T_{SmCTB-SHSmA}$ ; filled diamonds  $T_{SmCTB-SHN}$ ; unfilled triangles  $T_{SmCTB-DHSmCTB-SH}$ ; filled triangles  $T_{SmCTB-DHNTB}$ ; crosses  $T_{SmXSmCTB-DH}$ .

In order to achieve this goal, we increased the interactions between the mesogenic moieties by increasing the structural anisotropy of the benzylideneaniline moiety in the  $CB6O.m$  series to obtain the  $CB6OIBeOm$  series [3]:



Again, we chose the hexyloxy spacer to impart the required molecular curvature and varied the terminal chain length,  $m = 1-10$ , to increase molecular inhomogeneity and further promote smectic behaviour. For short terminal chain lengths,  $m = 1-6$ , a transition between the conventional and twist-bend nematic phases was observed, whereas for  $m \geq 7$ , the  $N_{TB}$  phase was extinguished and up to four lamellar phases were found below the N phase (Figure 14). The layer spacings in all the smectic phases corresponded to approximately the molecular length. The lowest temperature lamellar phase, seen for most of the homologues,  $m = 2, 4-10$ , is a hexatic-type smectic phase, designated HexI, in which the molecules tilt towards the apex of the local in-plane hexagons. The three higher temperature smectic phases showed liquid-like ordering of the molecules within the layers, and the changes in optical texture seen on cooling from the nematic phase are shown in Figure 15a. The highest temperature smectic phase was optically uniaxial and assigned as a SmA phase. On cooling, a schlieren texture developed, and at the transition there was no change in layer spacing, only the layer thermal expansion coefficient differed between the phases, both negative in sign, suggesting both phases to be orthogonal. The observed schlieren texture suggested that this phase was the biaxial smectic A,  $SmA_b$ , phase, in which molecular rotation around the long axis is, to some degree, frozen and this assignment is consistent with the increase in

layer spacing on cooling. The absence of a polar response under an electric field indicated that in the  $\text{SmA}_b$  phase the dipole moments of the molecules must be locally compensated. On cooling the  $\text{SmA}_b$  phase into the lowest temperature liquid-like smectic phase, the layer spacing decreased continuously suggesting a transition to a tilted phase, but surprisingly a homeotropic optical texture was restored (Figure 15a) ruling out the possibility of a simple all-in-one plane synclonic or anticlinic  $\text{SmC}$  phase. The observed optical uniaxiality of this tilted phase strongly suggested an averaging of the molecular orientations arising from the formation of a helical structure. This view was supported using soft X-ray resonant scattering which revealed that, at the transition from the  $\text{SmA}$  phase, a resonant Bragg peak developed corresponding to a pitch length of around 150 Å decreasing to around 117 Å at the transition to the  $\text{HexI}$  phase (Figure 15b). The pitch length was incommensurate with the layer thickness, corresponding to around 3–4 smectic layer distances. This heliconical smectic C phase was designated as the  $\text{SmC}_{\text{TB}}$  phase and the molecular arrangement within the phase is shown schematically in Figure 16. The  $\text{SmC}_{\text{TB}}$  phase does not appear optically active suggesting that essentially free molecular rotation occurs around the long molecular axis such that the biaxiality is too weak to give rise to detectable layer chirality, and it is known that optical activity is negligible in chiral smectic phases in which the pitch length is much shorter than the wavelength of light as is the case here. A resonant peak was also detected in the  $\text{HexI}$  phase corresponding to a pitch length of around 100 Å, around 2.2 smectic layer spacings, and this was essentially temperature independent (Figure 15b). The  $\text{HexI}$  phase showed a weakly birefringent texture (Figure 15a) with optically active domains and gave a circular dichroism signal around the absorption band of the material. This optical activity was attributed to the strongly inhomogeneous electron distribution across the layer and the tilting of the biaxial molecules, i.e., layer chirality (Figure 17); this originates given that the bent molecules are tilted with respect to the layer normal and changing the direction of the bend vector with respect to the tilt plane results in a non-superimposable mirror image. The morphology of the  $\text{HexI}$  phase was studied using atomic force microscopy revealing uniformly oriented entangled filaments with an average diameter of around 50 nm. These filaments had a uniform twist sense over areas of micron dimensions. The  $\text{HexI}$  phase, therefore, exhibits structural chirality at different length-scales, namely layer chirality, nanoscale helices and mesoscopic helical filaments, and strongly resembles the  $\text{B}_4$  phase but this has an internal crystalline structure [28,93] whereas the  $\text{HexI}$  phase does not. It should be noted that although all the smectic phases are single layer type with  $d\sim l$ , in the  $\text{HexI}$  phase, an additional, very weak diffraction signal corresponding to  $2l$  periodicity was detected [94], evidencing a tendency towards bilayer packing driven by a small imbalance in the density of the cyano groups at consecutive layer interfaces. Based on the RSoXS pattern it was deduced that the structure of  $\text{HexI}$  phase is anticlinic with a longer helix superimposed on that of the bilayer unit. A comparison of the calculated and experimental RSoXS patterns suggests that the layer chirality is coupled to the handedness of the longer superimposed helix.

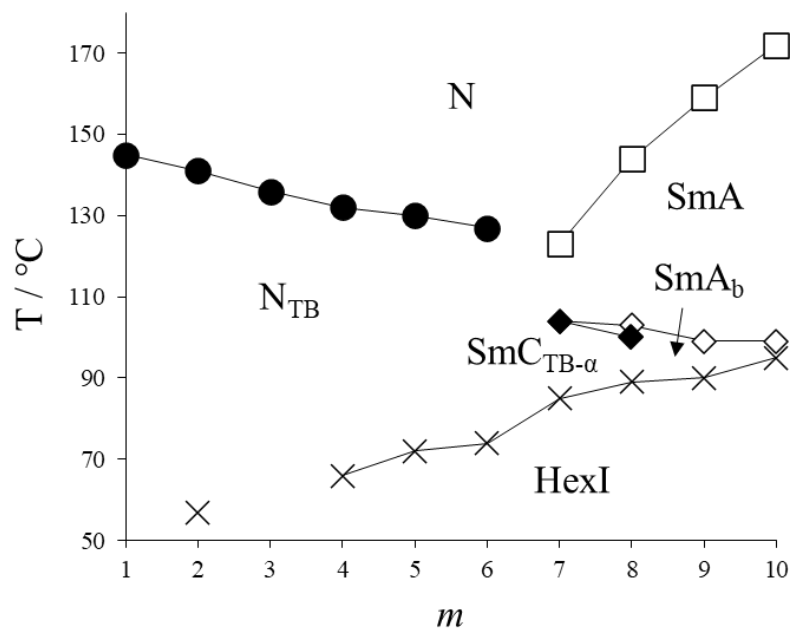


**Figure 14.** The dependence of the transition temperatures on the length of the terminal chain,  $m$ , for the CB6OIBeOm series [3]. The N-I transition temperatures have not been shown in order to enlarge the other phase regions. The melting points have been omitted for the sake of clarity. Filled circles denote  $T_{N_{TB}N}$ ; unfilled squares  $T_{SmAN}$ ; unfilled diamonds  $T_{SmAbSmA}$ ; filled diamonds  $T_{SmCTB-\alpha SmAb}$ ; crosses  $T_{HexI}$ .

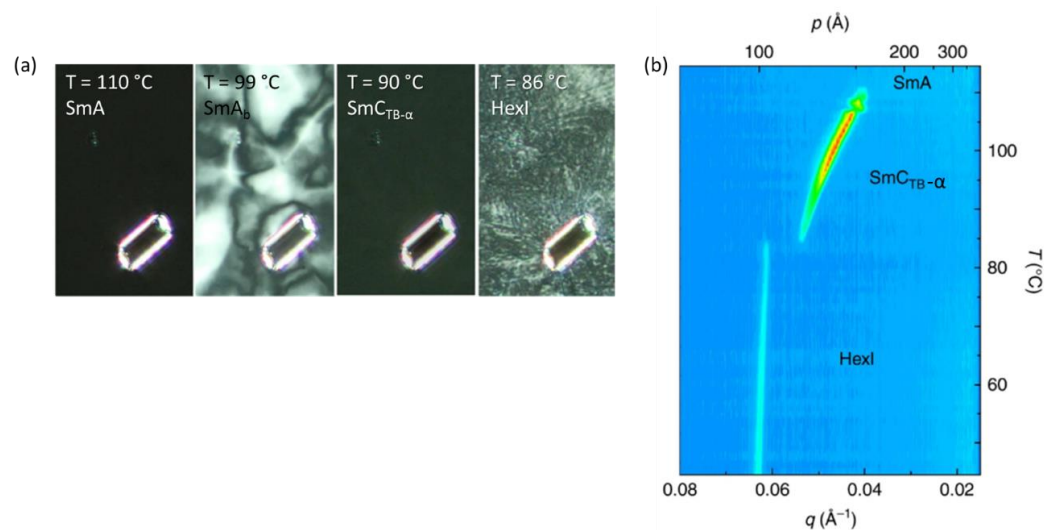


**Figure 15.** (a) The optical textures observed between crossed polarisers for CB6OIBeO8 on cooling in an homeotropic cell. A glass bead has been used to indicate that the textures represent the same area of the slide; (b) temperature dependence of the resonant soft X-ray diffraction signal for CB6OIBeO7 recorded on cooling (taken from [3]).



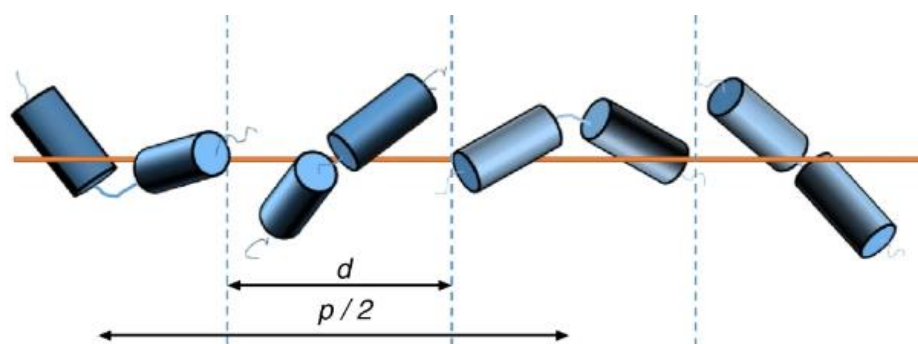


**Figure 16.** A schematic representation of the molecular arrangement within the  $\text{SmC}_{\text{TB}}$  phase (taken from [3]).

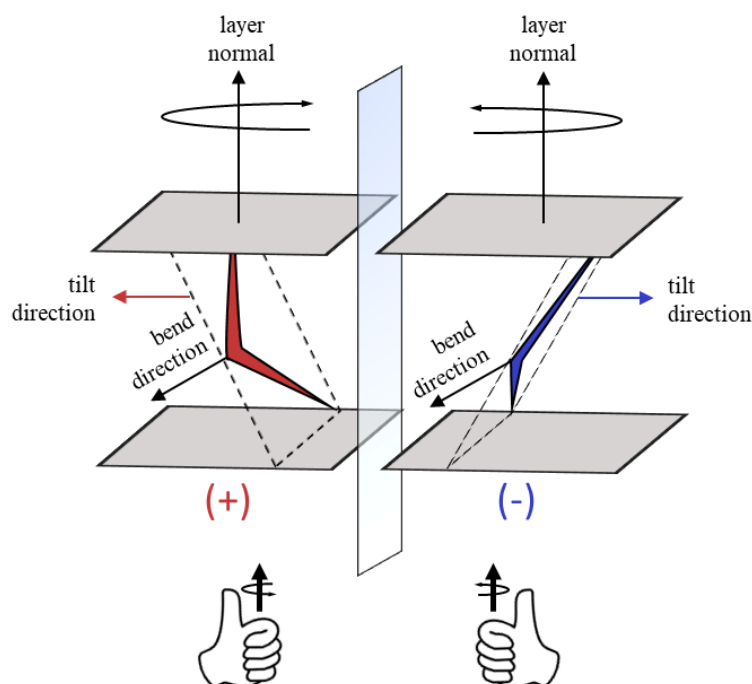


**Figure 17.** A sketch showing layer chirality in a tilted phase consisting of bent molecules.

The heliconical  $\text{SmC}_{\text{TB}}$  phase was the first unambiguous example of a short pitch helical structure consisting of achiral dimers arranged into a lamellar phase. The driving force for the spontaneous formation of this short-pitch length helical structure is presumably the anomalously low-bend elastic constant which may be attributed to the bent molecules. Such a view is supported by the striped optical texture observed in the  $\text{SmC}_{\text{TB}}$  phase which, by analogy to the interpretation of the striped texture observed for the  $\text{N}_{\text{TB}}$  phase [95], suggests that the bend elastic constant is very low. In chiral systems, the  $\text{SmC}\alpha^*$  phase, found between the  $\text{SmA}^*$  and  $\text{SmC}^*$  phases, has a similarly short pitch length incommensurate with the layer spacing, typically between 5 and 8 smectic layers, and has a small tilt angle [96,97]. In this structure, the helix formation relieves the frustration in systems in which next nearest interactions favour antiparallel tilt. Given the similarity in structure between the  $\text{SmC}_{\text{TB}}$  phase shown by  $\text{CB6OIBeO}_m$  series and the  $\text{SmC}\alpha^*$  phase, we designate this  $\text{SmC}_{\text{TB}}$  variant as the  $\text{SmC}_{\text{TB}-\alpha}$  phase. Polar bent core molecules had also been reported to show a short pitch heliconical smectic phase designated  $\text{Sm}(\text{CP})^{\text{hel}}$  and this is thought to be associated with the growth of polar order at the anticlinic-synclinic transition in smectic phases with a small tilt angle [98–100]. Again, the pitch length was incommensurate with the layer spacing, and typically around three-layer thicknesses. Earlier, liquid crystal phases containing helices of both handedness had been reported for

bent-core liquid crystals by Sekine et al. [101], although this was later assigned as a  $B_4$  phase, and technically crystalline in nature.

We saw earlier that CB6O.10 was the shortest member of the CB6O.*m* series to exhibit a smectic phase (Figure 13) and this was subsequently studied in detail and assigned as a  $Sm_{C_{TB}}$  phase [94]. The  $Sm_{C_{TB}}-N_{TB}$  transition was clearly observed using DSC, but was not associated with changes in optical textures. This suggested that in both phases there was a similar averaging of molecular orientation due to the formation of a helix. Only a small change in birefringence was seen at the  $Sm_{C_{TB}}-N_{TB}$  transition, evidencing that the conical angle in both phases is similar, and estimated to be  $15^\circ$ . Non-resonant XRD measurements revealed the layer spacing in the smectic phase to be almost two molecular lengths suggesting a bilayer arrangement with the molecules arranged head-to-head within a layer. A resonant signal was evident in the RSoXS pattern of the  $N_{TB}$  phase associated with the helix, and showed that the pitch length decreased with decreasing temperature (Figure 18). At the  $N_{TB}-Sm_{C_{TB}}$  transition, the resonant signal ( $q_4$  in Figure 18) locks at approximately four molecular lengths and this persists for several degrees below the phase transition. This signal was purely resonant indicating it was associated with the helical structure. A signal associated with the bilayer structure was also observed but off-scale in Figure 18. The continuous evolution of structure at the  $N_{TB}-Sm_{C_{TB}}$  transition suggested that in the smectic phase just below the transition, the molecules in adjacent layers are azimuthally rotated by exactly  $90^\circ$  on the tilt cone and this may be described as an ideal clock structure (see Figure 19a). A model used to estimate the intensities of the RSoXS signals suggested that deeper in the phase, the structure may be described as a distorted clock with  $\delta$  between  $60-70^\circ$  (Figure 19b). In such an arrangement the helical pitch is commensurate with two smectic bilayer spacings; in other words, approximately four molecular lengths. On cooling the  $Sm_{C_{TB}}$  phase, the resonant signal ( $q_4$ ) split symmetrically into two resonant signals, ( $q_4 + q_m$ ) and ( $q_4 - q_m$ ), with the former much more intense. This splitting increased with decreasing temperature. A very weak signal at  $2q_m$  was also observed.

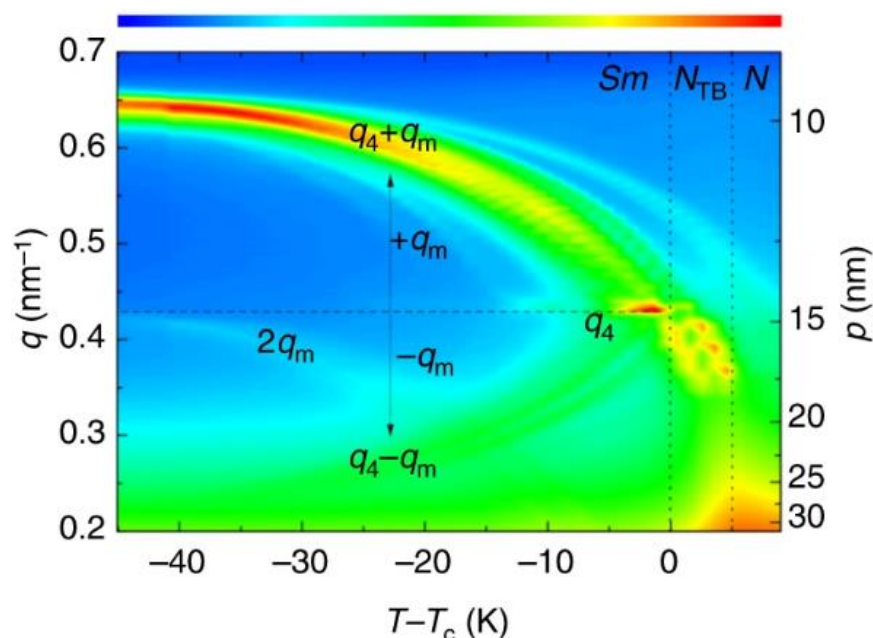
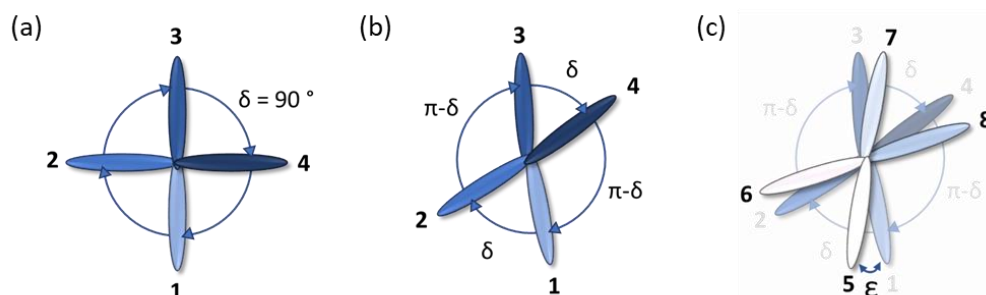


Figure 18. The resonant soft-X-ray scattering pattern for CB6O.10 (taken from [94]).



**Figure 19.** Schematic representations of the  $\text{SmC}_{\text{TB}}$  phases using the clock model in which the ellipse represents the direction of the tilt projected onto the layer plane. (a) The ideal clock in which molecules rotate on the tilt cone by exactly  $90^\circ$  between consecutive layers. (b) The distorted clock in which the azimuthal angle between the projections of the long molecular axis in adjacent layers onto the smectic plane is no longer  $90^\circ$ . (c) A change in azimuthal angle to the adjacent layer causing the four-layer unit cell to rotate giving an additional helical structure.

The RSoXS pattern of either a smectic phase in which the basic four-layer unit repeats with a regular distribution of the molecules on the tilt cone (Figure 19a,b), or the all-in-one-plane bilayer structure with alternating synclincic and anticlinic interfaces between the constituent molecular layers, should contain only the signal  $q_4$  and its harmonics. The splitting of the  $q_4$  signal in Figure 18 indicated that an additional modulation, with a longer periodicity, is superimposed over the basic four-layer unit. It was noted that the pattern shown in Figure 18 was very similar to that seen for the  $\text{SmC}_{\text{FI2}}^*$  phase observed over narrow temperature ranges between anticlinic and synclincic  $\text{SmC}^*$  phases in chiral rod-like materials [102]. The  $\text{SmC}_{\text{FI2}}^*$  has also a four-layer unit cell in which the molecules in consecutive layers form a distorted helix such that the azimuthal angle,  $\delta$ , between the projections of the long molecular axis in adjacent layers on to the smectic plane is not  $90^\circ$  (Figure 19b). In addition, the azimuthal angle increases by some amount,  $\epsilon$ , with respect to the adjacent layer causing the four-layer unit cell to rotate giving an additional helical structure (Figure 19c). The smectic phase shown by CB6O.10 is thought to be similar to this structure, but it should be stressed that given the molecules are achiral, the driving force for its formation must be different than in case of the  $\text{SmC}_{\text{FI2}}^*$  phase. We termed this phase  $\text{SmC}_{\text{TB-DH}}$  where DH indicates double helix and show the structure as a distorted clock in Figure 19c and schematically in Figure 20. An important difference to the structure of the  $\text{SmC}_{\text{FI2}}^*$  phase is that in the  $\text{SmC}_{\text{TB-DH}}$  phase, the modulation superimposed on the basic four-layer unit is much stronger, and similar to the basic modulation, is on the nanometre scale. A model used to predict the RSoXS signal intensities has shown that the handedness of the short four-layer structure determines that of the longer helical modulation. The angle  $\delta$  is essentially temperature independent whereas  $\epsilon$  is strongly temperature dependent giving rise to the evolution of the helical structure shown in Figure 20. Close to the  $\text{N}_{\text{TB}}\text{-SmC}_{\text{TB-DH}}$  transition, we see an almost ideal clock four-layer structure (Figure 19a) but as  $\epsilon$  increases on decreasing temperature, the structure evolves towards an anticlinic arrangement. We should also note that the bent nature of the molecules introduces another level of structural chirality, the sign of which is defined by the relative orientation of three vectors: the layer normal, the tilt projection onto the smectic layer, and the molecular bend direction. This structural chirality is referred to as layer chirality and was described earlier (Figure 17) [92]. Presumably the sign of the layer chirality is coupled to the handedness of the four-layer basic unit and hence to the longer, superimposed helix. We have seen earlier that in the  $\text{N}_{\text{TB}}$  phase steric interactions drive the formation of the helical structure, and the pitch length decreases on reducing the temperature. On cooling into the  $\text{SmC}_{\text{TB-DH}}$  phase an ideal four-layer clock helical structure forms, in which the azimuthal tilt angle changes by  $90^\circ$  on passing from layer to layer. As the temperature is reduced, the competition increases between the tendency to twist and the entropy-driven tendency for molecules to remain in one tilt plane which allows for easier molecular movement along the layer

normal, and thus, the structure continuously evolves from the four-layer clock to an almost anticlinic bilayer arrangement. By comparison, in chiral materials a series of discontinuous phase transitions have been observed rather than a continuous evolution of structure [96].

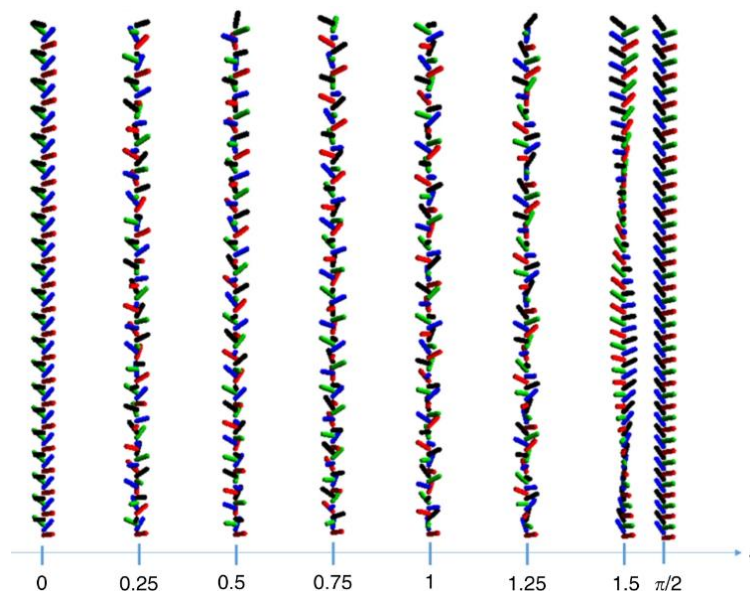


**Figure 20.** A schematic representation of the evolution of the four-layer structure in the  $\text{SmC}_{\text{TB-DH}}$  phase on increasing  $\mathcal{E}$ , the difference between the azimuthal angle between adjacent layers. For clarity the tilt angle has been increased. (Taken from [94]).

A study of the longer homologues of the  $\text{CB6O}_m$  series, ( $m = 12, 14, 16, 18$ ) revealed a sequence of four smectic phases:  $\text{SmA}—\text{SmC}_{\text{TB-SH}}—\text{SmC}_{\text{TB-DH}}—\text{SmX}$  below the I or N phase (Figure 13) [91]. The lowest temperature phase,  $\text{SmX}$ , was not studied in detail, but its X-ray diffraction pattern indicated that it is a hexatic-type smectic phase. The  $\text{SmA}$  phase was optically uniaxial (Figure 21) and the layer spacing corresponded to two molecular lengths indicating a bilayer structure in which the cyano groups are concentrated at alternating interfaces, as seen for  $\text{CB6O}_{10}$ . X-ray diffraction revealed that the  $\text{SmA}$ ,  $\text{SmC}_{\text{TB-SH}}$ , and  $\text{SmC}_{\text{TB-DH}}$  phases are liquid-like in terms of in-plane ordering. The  $\text{SmC}_{\text{TB-SH}}$  phase was optically biaxial whereas the  $\text{SmC}_{\text{TB-DH}}$  is optically uniaxial (Figure 21). The RSoXS pattern of the  $\text{SmC}_{\text{TB-SH}}$  phase contained a resonant peak corresponding to four molecular layers and its position was temperature independent, and using non-resonant XRD, a bilayer structure was observed. SH is used to indicate that the  $\text{SmC}_{\text{TB-SH}}$  phase is characterised by having a single helix. On entering the  $\text{SmC}_{\text{TB-DH}}$  phase, symmetric satellites of the resonant peak developed indicating an additional modulation superimposed on the basic four-layer helix. Unlike the continuous development of this peak splitting seen in the RSoXS pattern for  $\text{CB6O}_{10}$ , the satellites' peaks change discontinuously with temperature, and this is thought to be associated with surface interactions. The  $\text{SmC}_{\text{TB-SH}}—\text{SmC}_{\text{TB-DH}}$  phase transition is not associated with a change in layer spacing as measured using non-resonant XRD, implying that the tilt angle does not change. The optical biaxiality of the  $\text{SmC}_{\text{TB-SH}}$  phase suggests a distorted clock structure for its four-layer unit cell (Figure 19b). In the optically uniaxial  $\text{SmC}_{\text{TB-DH}}$  phase an additional shift in azimuthal angle,  $\mathcal{E}$ , between consecutive layers gives rise to a longer pitch-length helical modulation superimposed on the basic 4-layer helical structure. This additional helix has a pitch length corresponding to around 16 layers deep into the  $\text{SmC}_{\text{TB-DH}}$  phase but as the temperature approaches the  $\text{SmC}_{\text{TB-SH}}—\text{SmC}_{\text{TB-DH}}$  transition, the pitch length jumps to around 46-layer distances. As we saw for  $\text{CB6O}_{10}$ , this change in the pitch length reflects the evolution of the structure from a bilayer towards a four-layer arrangement with alternating synclinic and anticlinic interfaces. The equal intensities of the satellite peaks in the RSoXS pattern for the  $\text{SmC}_{\text{TB-DH}}$  phase imply that the angle  $\delta$  must be small such that the basic four-layer unit is a strongly distorted clock in

which alternating interfaces approach synclinic and anticlinic arrangements. A study of the  $\text{SmC}_{\text{TB-DH}}-\text{SmC}_{\text{TB-SH}}$  transition using optical microscopy revealed selective reflection colours covering the whole optical spectrum at temperatures very close to the transition, which indicated unwinding of the additional helix of the  $\text{SmC}_{\text{TB-DH}}$  phase (Figure 22) [91]. The selective reflection of light occurs when the pitch of the helix, as it unwinds, becomes comparable to the wavelength of visible light, and this was the first observation of such behaviour for achiral liquid crystals.

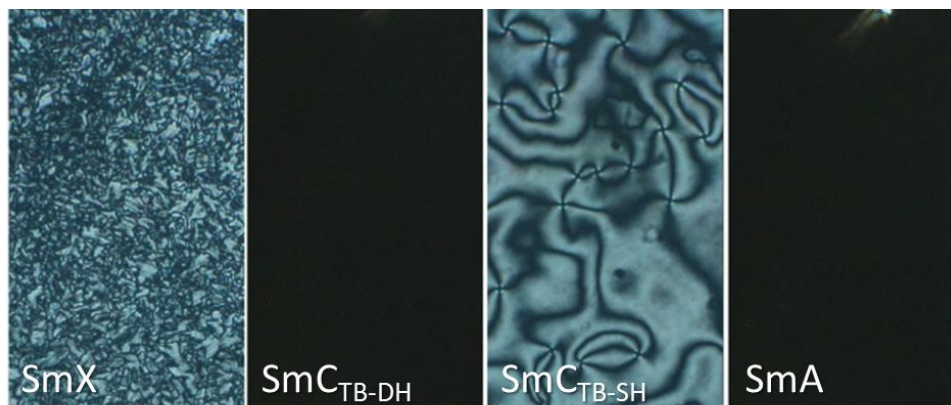


**Figure 21.** Optical textures of CB6O.14 observed between crossed polarizers in a 3  $\mu\text{m}$  thick cell with homeotropic anchoring (taken from [91]).

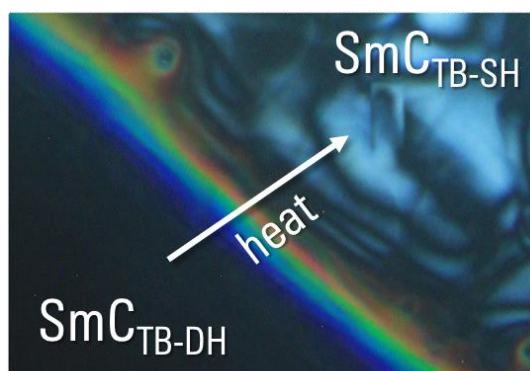
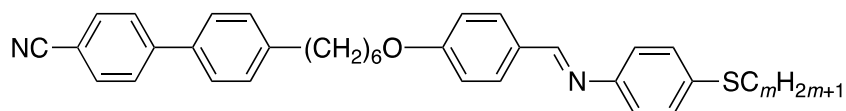


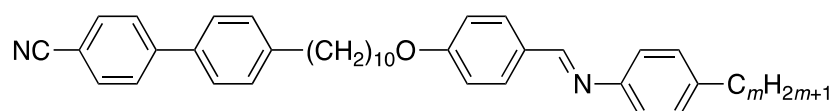
**Figure 22.** The optical texture shown by CB6O.12 taken in a 3  $\mu\text{m}$  thick cell with homeotropic anchoring at the  $\text{SmC}_{\text{TB-DH}}-\text{SmC}_{\text{TB-SH}}$  transition showing selective reflection. The colours appear simultaneously because of a small temperature gradient in the sample. (Taken from [91]).

The corresponding dimers containing a thioether-linked terminated chain,  $\text{CB6O.Sm}$ , [103]



also show the  $\text{SmC}_{\text{TB-DH}}-\text{SmC}_{\text{TB-SH}}$  transition for  $m > 13$ , but the monotropic nature of these phases prevented their detailed study. This series of bent dimers also showed the helical filament  $\text{B}_4$  phase described earlier.

To investigate the effects of increasing the spacer length on the formation of the heliconical  $\text{SmC}_{\text{TB}}$  phases, we studied the properties of the 1-(4-cyanobiphenyl-4'-yl)-10-(4-alkylaniline-benzylidene-4'-oxy)decans ( $\text{CB10O.m}$ ) [104]:



with the terminal chain length,  $m = 1-10, 12, 14, 16$  and  $18$ . The CB100. $m$  series shows a rich phase polymorphism including the N and N<sub>TB</sub> phases, and six different smectic phases (Figure 23). All the homologues showed the conventional N phase. For the shortest members,  $m = 1-3$ , the N<sub>TB</sub> phase was seen. An intercalated SmC<sub>A</sub> phase emerged for CB100.3, and for  $m = 4-6$  the N<sub>TB</sub> phase was extinguished and a direct SmC<sub>A</sub>-N transition observed. The N<sub>TB</sub> phase reemerged with CB100.7, and the SmC<sub>A</sub> phase extinguished after  $m = 8$ . The homologues with  $m = 9$  and  $10$  were exclusively nematogenic, showing both N and N<sub>TB</sub> phases. Smectic behaviour re-emerged at  $m = 12$ , and the longer homologues exhibited heliconical SmC<sub>TB</sub> phases. This pattern of behaviour has clear similarities to that seen for the CBO4O. $m$  series (Figure 5) for which smectic phases were observed for short and long terminal chain lengths and solely nematic behaviour for intermediate chain lengths [18]. For the CBO4O. $m$  series, this was interpreted in terms of the change in the structure of the smectic phases on increasing chain length from being interdigitated to intercalated (Figure 6). A similar explanation accounts for the behaviour seen for the CB100. $m$  series except that with increasing  $m$  we now see a switch from intercalated to interdigitated bilayer smectic phases. Three homologues ( $m = 12, 14, 16$ ) show SmC<sub>TB-SH</sub> and SmC<sub>TB-DH</sub> phases whereas for the longest homologue only the SmC<sub>TB-SH</sub> phase is seen, presumably the transition to the SmC<sub>TB-DH</sub> phase is precluded by the formation of the underlying SmY phase. As described for the CB6O. $m$  series, the SmC<sub>TB-SH</sub> phase is optically biaxial implying a strongly distorted clock arrangement (Figure 19b) whereas the SmC<sub>TB-DH</sub> phase is optically uniaxial, given the additional modulation superimposed on the basic four-layer structure leading to space-averaging of the azimuthal positions of the molecules along the layer normal (Figure 20). It is interesting to note that there is no apparent change in layer spacing at the SmC<sub>TB-SH</sub>-SmC<sub>TB-DH</sub> transition implying the tilt angle is similar in both. The striking difference in the nature of the smectic phases shown by  $m = 3-8$ , and  $m \geq 12$  is revealed in the behaviour of an approximately equimolar mixture of homologues with  $m = 6$  and  $16$  that exhibited the N<sub>TB</sub> phase over a broad temperature range although neither individual component does. This shows that the intercalated and interdigitated smectic phases are incompatible and destabilised in the mixture, revealing the underlying N<sub>TB</sub> phase.

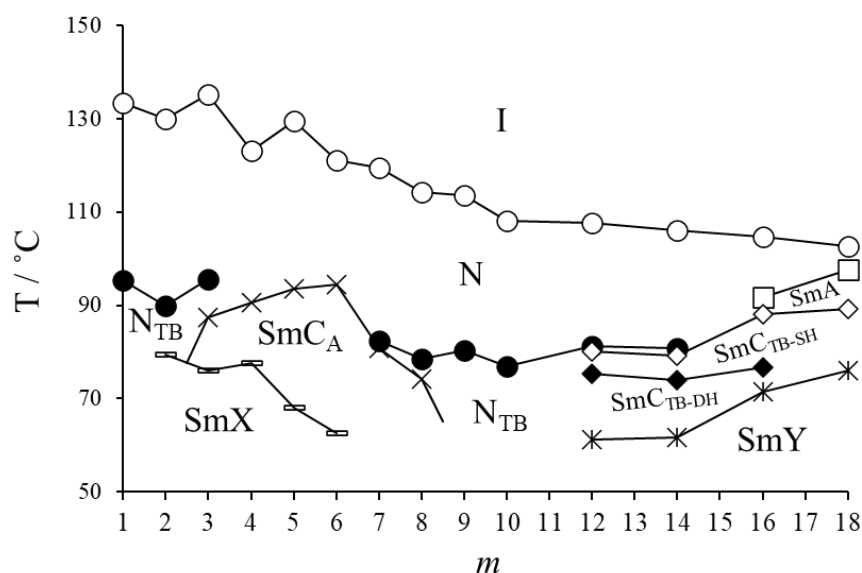


**Figure 23.** The dependence of the transition temperatures on the length of the terminal chain,  $m$ , for the CB100. $m$  series [104]. The melting points have been omitted for the sake of clarity. The dependence of the transition temperatures on the length of the terminal chain,  $m$ , for the CB100. $m$  series [104]. The melting points have been omitted for the sake of clarity. Unfilled circles denoted  $T_{NI}$ ; filled circles  $T_{NTB}$ ; crosses  $T_{SmCN/N_{TB}}$ ; dashes  $T_{SmX}$ ; squares  $T_{SmA}$ ; unfilled diamonds  $T_{SmC_{TB-SH}}$ ; filled diamonds  $T_{SmC_{TB-DH}}$ ; stars  $T_{SmY}$ .

## 7. Summary and Outlook

In this review we have discussed the relationships between the smectic behaviour of liquid crystal dimers and their molecular structures. These are dominated by the average shape of the molecule and markedly different behaviour is seen for bent-odd membered dimers than for linear even-membered dimers. For symmetric dimers there is a strong preference for the formation of monolayer smectic phases driven apparently by the incompatibility between the mixing of the spacers and terminal chains. This may be overcome for nonsymmetric dimers for which intercalated and interdigitated smectic phases are observed depending on the relative lengths of the spacers and terminal chains. The stronger tendency of odd-membered dimers to exhibit tilted phases is attributed to the difficulty associated with the packing of their bent shape into orthogonal phases. By adjusting the molecular curvature, it is possible to drive the formation of spontaneously chiral twist-bend smectic phases, and to date, we have reported three variants of the  $\text{SmC}_{\text{TB}}$  phase. In the  $\text{SmC}_{\text{TB-}\alpha}$  phase, the helical pitch length is incommensurate with the layer spacing and the phase is optically uniaxial. In the  $\text{SmC}_{\text{TB-SH}}$  phase the helical pitch corresponds to approximately four molecular lengths, and may be described by the distorted clock model and the phase is optically biaxial. The  $\text{SmC}_{\text{TB-DH}}$  phase has an additional helical modulation described by the rotation of the basic four-layer units by a temperature dependent angle, and thus is optically uniaxial. To date, the twist-bend arrangement has only been reported for either monolayer or bilayer smectic phases, and not for intercalated structures. We anticipate, however, the discovery of further variants of the  $\text{SmC}_{\text{TB}}$  phase as a wider expanse of molecular structure space is explored. More widely, the spontaneous formation of chiral structures with multiple different levels of chirality by achiral molecules is an area of intense global interest and of fundamental importance in the physical and biological sciences. The study of liquid crystal dimers has an exciting and vibrant future!

**Author Contributions:** All the authors have made a substantial, and intellectual contribution to the work and approved it for publication. All authors have read and agreed to the published version of the manuscript.

**Funding:** This research received no external funding.

**Acknowledgments:** The authors gratefully acknowledge Professor Nataša Vaupotič for her central role in the interpretation of the resonant soft X-ray scattering (RSOXS) data and the preparation of the original figures. The authors also wish to thank Ewan Cruickshank for many helpful discussions.

**Conflicts of Interest:** The authors declare no conflict of interest.

## References

1. Cestari, M.; Diez-Berart, S.; Dunmur, D.A.; Ferrarini, A.; de la Fuente, M.R.; Jackson, D.J.B.; Lopez, D.O.; Luckhurst, G.R.; Perez-Jubindo, M.A.; Richardson, R.M.; et al. Phase behavior and properties of the liquid-crystal dimer 1'',7''-bis(4-cyanobiphenyl-4'-yl) heptane: A twist-bend nematic liquid crystal. *Phys. Rev. E* **2011**, *84*, 031704. [[CrossRef](#)] [[PubMed](#)]
2. Dozov, I. On the spontaneous symmetry breaking in the mesophases of achiral banana-shaped molecules. *Europhys. Lett.* **2001**, *56*, 247–253. [[CrossRef](#)]
3. Abberley, J.P.; Killah, R.; Walker, R.; Storey, J.M.D.; Imrie, C.T.; Salamonczyk, M.; Zhu, C.H.; Gorecka, E.; Pocięcha, D. Helical smectic phases formed by achiral molecules. *Nat. Commun.* **2018**, *9*, 228. [[CrossRef](#)] [[PubMed](#)]
4. Imrie, C.T.; Henderson, P.A. Liquid crystal dimers and oligomers. *Curr. Opin. Colloid Interface Sci.* **2002**, *7*, 298–311. [[CrossRef](#)]
5. Imrie, C.T.; Henderson, P.A. Liquid crystal dimers and higher oligomers: Between monomers and polymers. *Chem. Soc. Rev.* **2007**, *36*, 2096–2124. [[CrossRef](#)]
6. Imrie, C.T.; Henderson, P.A.; Yeap, G.Y. Liquid crystal oligomers: Going beyond dimers. *Liq. Cryst.* **2009**, *36*, 755–777. [[CrossRef](#)]
7. Attard, G.S.; Garnett, S.; Hickman, C.G.; Imrie, C.T.; Taylor, L. Asymmetric dimeric liquid-crystals with charge-transfer groups. *Liq. Cryst.* **1990**, *7*, 495–508. [[CrossRef](#)]
8. Griffin, A.C.; Britt, T.R. Effect of molecular-structure on mesomorphism.12. Flexible-center siamese-twin liquid-crystalline diesters—A prepolymer model. *J. Am. Chem. Soc.* **1981**, *103*, 4957–4959. [[CrossRef](#)]
9. Vorlander, D. On the nature of carbon chains in crystalline-fluid substances. *Z. Phys. Chem.* **1927**, *126*, 449–472.
10. Date, R.W.; Imrie, C.T.; Luckhurst, G.R.; Seddon, J.M. Smectogenic dimeric liquid-crystals—The preparation and properties of the alpha,omega-bis(4-n-alkylanilinebenzylidene-4'-oxy)alkane. *Liq. Cryst.* **1992**, *12*, 203–238. [[CrossRef](#)]

11. Smith, G.W.; Gardlund, Z.G.; Curtis, R.J. Phase-transitions in mesomorphic benzylideneanilines. *Mol. Cryst. Liq. Cryst.* **1973**, *19*, 327–330. [[CrossRef](#)]
12. Date, R.W.; Luckhurst, G.R.; Shuman, M.; Seddon, J.M. Novel modulated hexatic phases in symmetrical liquid-crystal dimers. *J. Phys II Fr.* **1995**, *5*, 587–605.
13. Imrie, C.T. Non-symmetric liquid crystal dimers: How to make molecules intercalate. *Liq. Cryst.* **2006**, *33*, 1449–1454. [[CrossRef](#)]
14. Henderson, P.A.; Niemeyer, O.; Imrie, C.T. Methylene-linked liquid crystal dimers. *Liq. Cryst.* **2001**, *28*, 463–472. [[CrossRef](#)]
15. Henderson, P.A.; Seddon, J.M.; Imrie, C.T. Methylene- and ether-linked liquid crystal dimers, I.I. Effects of mesogenic linking unit and terminal chain length. *Liq. Cryst.* **2005**, *32*, 1499–1513. [[CrossRef](#)]
16. Henderson, P.A.; Imrie, C.T. Methylene-linked liquid crystal dimers and the twist-bend nematic phase. *Liq. Cryst.* **2011**, *38*, 1407–1414. [[CrossRef](#)]
17. Hogan, J.L.; Imrie, C.T.; Luckhurst, G.R. Asymmetric dimeric liquid-crystals—The preparation and properties of the  $\alpha$ -(4-cyanobiphenyl-4'-oxy)- $\omega$ -(4-*n*-alkylanilinebenzylidene-4'-oxy)hexanes. *Liq. Cryst.* **1988**, *3*, 645–650. [[CrossRef](#)]
18. Attard, G.S.; Date, R.W.; Imrie, C.T.; Luckhurst, G.R.; Roskilly, S.J.; Seddon, J.M.; Taylor, L. Nonsymmetrical dimeric liquid-crystals—The preparation and properties of the alpha-(4-cyanobiphenyl-4'-yloxy)-omega-(4-*n*-alkylanilinebenzylidene-4'-oxy)alkanes. *Liq. Cryst.* **1994**, *16*, 529–581. [[CrossRef](#)]
19. Park, J.W.; Bak, C.S.; Labes, M.M. Effects of molecular complexing on properties of binary nematic liquid-crystal mixtures. *J. Am. Chem. Soc.* **1975**, *97*, 4398–4400. [[CrossRef](#)]
20. Cladis, P.E. The re-entrant nematic, enhanced smectic-a phases and molecular composition. *Mol. Cryst. Liq. Cryst.* **1981**, *67*, 833–847. [[CrossRef](#)]
21. Blatch, A.E.; Fletcher, I.D.; Luckhurst, G.R. The intercalated smectic A phase—The liquid-crystal properties of the alpha(4-cyanobiphenyl-4'-yloxy)-omega-(4-alkyloxycinnamoate)alkanes. *Liq. Cryst.* **1995**, *18*, 801–809. [[CrossRef](#)]
22. Takahashi, Y.; Takezoe, H.; Fukuda, A.; Komura, H.; Watanabe, J. Simple method for confirming the antiferroelectric structure of smectic liquid-crystals. *J. Mater. Chem.* **1992**, *2*, 71–73. [[CrossRef](#)]
23. Le Masurier, P.J.; Luckhurst, G.R. Structural studies of the intercalated smectic C phases formed by the non-symmetric alpha-(4-cyanobiphenyl-4'-yloxy)-omega-(4-alkylaniline-benzylidene-4'-oxy) alkane dimers using EPR spectroscopy. *J. Chem. Soc. Faraday Trans.* **1998**, *94*, 1593–1601. [[CrossRef](#)]
24. Walker, R.; Pocięcha, D.; Faidutti, C.; Perkovic, E.; Storey, J.M.D.; Gorecka, E.; Imrie, C.T. Remarkable stabilisation of the intercalated smectic phases of nonsymmetric dimers by tert-butyl groups. *Liq. Cryst.* **2022**, *49*, 969–981. [[CrossRef](#)]
25. Watanabe, J.; Komura, H.; Niiori, T. Thermotropic liquid-crystals of polyesters having a mesogenic 4,4-benzoate unit—Smectic mesophase properties and structures in dimeric model compounds. *Liq. Cryst.* **1993**, *13*, 455–465. [[CrossRef](#)]
26. Reddy, R.A.; Tschierske, C. Bent-core liquid crystals: Polar order, superstructural chirality and spontaneous desymmetrisation in soft matter systems. *J. Mater. Chem.* **2006**, *16*, 907–961. [[CrossRef](#)]
27. Bialecka-Florjanczyk, E.; Sledzinska, I.; Gorecka, E.; Przedmojski, J. Odd-even effect in biphenyl-based symmetrical dimers with methylene spacer—Evidence of the B4 phase. *Liq. Cryst.* **2008**, *35*, 401–406. [[CrossRef](#)]
28. Hough, L.E.; Jung, H.T.; Kruerke, D.; Heberling, M.S.; Nakata, M.; Jones, C.D.; Chen, D.; Link, D.R.; Zasadzinski, J.; Heppke, G.; et al. Helical Nanofilament Phases. *Science* **2009**, *325*, 456–460. [[CrossRef](#)] [[PubMed](#)]
29. Le, K.V.; Takezoe, H.; Araoka, F. Chiral Superstructure Mesophases of Achiral Bent-Shaped Molecules—Hierarchical Chirality Amplification and Physical Properties. *Adv. Mater. Interfaces* **2017**, *29*, 1602737. [[CrossRef](#)]
30. Borshch, V.; Kim, Y.K.; Xiang, J.; Gao, M.; Jakli, A.; Panov, V.P.; Vij, J.K.; Imrie, C.T.; Tamba, M.G.; Mehl, G.H.; et al. Nematic twist-bend phase with nanoscale modulation of molecular orientation. *Nat. Commun.* **2013**, *4*, 2635. [[CrossRef](#)] [[PubMed](#)]
31. Zhu, C.H.; Tuchband, M.R.; Young, A.; Shuai, M.; Scarbrough, A.; Walba, D.M.; MacLennan, J.E.; Wang, C.; Hexemer, A.; Clark, N.A. Resonant Carbon K-Edge Soft X-ray Scattering from Lattice-Free Helical Molecular Ordering: Soft Dilative Elasticity of the Twist-Bend Liquid Crystal Phase. *Phys. Rev. Lett.* **2016**, *116*, 147803. [[CrossRef](#)] [[PubMed](#)]
32. Dunmur, D.A. Anatomy of a Discovery: The Twist-Bend Nematic Phase. *Crystals* **2022**, *12*, 309. [[CrossRef](#)]
33. Sepelj, M.; Lesac, A.; Baumeister, U.; Diele, S.; Nguyen, H.L.; Bruce, D.W. Intercalated liquid-crystalline phases formed by symmetric dimers with an alpha,omega-diiminoalkylene spacer. *J. Mater. Chem.* **2007**, *17*, 1154–1165. [[CrossRef](#)]
34. Panov, V.P.; Nagaraj, M.; Vij, J.K.; Panarin, Y.P.; Kohlmeier, A.; Tamba, M.G.; Lewis, R.A.; Mehl, G.H. Spontaneous Periodic Deformations in Nonchiral Planar-Aligned Bimesogens with a Nematic-Nematic Transition and a Negative Elastic Constant. *Phys. Rev. Lett.* **2010**, *105*, 167801. [[CrossRef](#)] [[PubMed](#)]
35. Ferrarini, A.; Luckhurst, G.R.; Nordio, P.L.; Roskilly, S.J. Understanding the unusual transitional behavior of liquid-crystal dimers. *Chem. Phys. Lett.* **1993**, *214*, 409–417. [[CrossRef](#)]
36. Ferrarini, A.; Luckhurst, G.R.; Nordio, P.L.; Roskilly, S.J. Understanding the dependence of the transitional properties of liquid crystal dimers on their molecular geometry. *Liq. Cryst.* **1996**, *21*, 373–382. [[CrossRef](#)]
37. Emerson, A.; Luckhurst, G.R.; Phippen, R.W. The average shapes of flexible mesogenic molecules—On the choice of reference frame. *Liq. Cryst.* **1991**, *10*, 1–14. [[CrossRef](#)]
38. Ferrarini, A.; Luckhurst, G.R.; Nordio, P.L.; Roskilly, S.J. Prediction of the transitional properties of liquid-crystal dimers—A molecular-field calculation based on the surface tensor parametrization. *J. Chem. Phys.* **1994**, *100*, 1460–1469. [[CrossRef](#)]
39. Paterson, D.A.; Abberley, J.P.; Harrison, W.T.; Storey, J.M.; Imrie, C.T. Cyanobiphenyl-based liquid crystal dimers and the twist-bend nematic phase. *Liq. Cryst.* **2017**, *44*, 127–146. [[CrossRef](#)]



40. Walker, R.; Pocięcha, D.; Strachan, G.J.; Storey, J.M.D.; Gorecka, E.; Imrie, C.T. Molecular curvature, specific intermolecular interactions and the twist-bend nematic phase: The synthesis and characterisation of the 1-(4-cyanobiphenyl-4-yl)-6-(4-alkylanilinebenzylidene-4-oxy)hexanes (CB6O.m). *Soft Matter*. **2019**, *15*, 3188–3197. [[CrossRef](#)]
41. Lu, Z.B.; Henderson, P.A.; Paterson, B.J.A.; Imrie, C.T. Liquid crystal dimers and the twist-bend nematic phase. The preparation and characterisation of the alpha,omega-bis(4-cyanobiphenyl-4'-yl) alkanedioates. *Liq. Cryst.* **2014**, *41*, 471–483. [[CrossRef](#)]
42. Paterson, D.A.; Gao, M.; Kim, Y.K.; Jamali, A.; Finley, K.L.; Robles-Hernandez, B.; Diez-Berart, S.; Salud, J.; de la Fuente, M.R.; Timimi, B.A.; et al. Understanding the twist-bend nematic phase: The characterisation of 1-(4-cyanobiphenyl-4'-yloxy)-6-(4-cyanobiphenyl-4'-yl)hexane (CB6OCB) and comparison with CB7CB. *Soft Matter*. **2016**, *12*, 6827–6840. [[CrossRef](#)] [[PubMed](#)]
43. Cruickshank, E.; Salamonczyk, M.; Pocięcha, D.; Strachan, G.J.; Storey, J.M.D.; Wang, C.; Feng, J.; Zhu, C.H.; Gorecka, E.; Imrie, C.T. Sulfur-linked cyanobiphenyl-based liquid crystal dimers and the twist-bend nematic phase. *Liq. Cryst.* **2019**, *46*, 1595–1609. [[CrossRef](#)]
44. Arakawa, Y.; Komatsu, K.; Feng, J.; Zhu, C.H.; Tsuji, H. Distinct twist-bend nematic phase behaviors associated with the ester-linkage direction of thioether-linked liquid crystal dimers. *Mater. Adv.* **2021**, *2*, 261–272. [[CrossRef](#)]
45. Arakawa, Y.; Komatsu, K.; Ishida, Y.; Igawa, K.; Tsuji, H. Carbonyl- and thioether-linked cyanobiphenyl-based liquid crystal dimers exhibiting twist-bend nematic phases. *Tetrahedron* **2021**, *81*, 131870. [[CrossRef](#)]
46. Arakawa, Y.; Tsuji, H. Selenium-linked liquid crystal dimers for twist-bend nematogens. *J. Mol. Liq.* **2019**, *289*, 111097. [[CrossRef](#)]
47. Lesac, A.; Baumeister, U.; Dokli, I.; Hamersak, Z.; Ivsic, T.; Kontrec, D.; Viskic, M.; Knezevic, A.; Mandle, R.J. Geometric aspects influencing N-N-TB transition—Implication of intramolecular torsion. *Liq. Cryst.* **2018**, *45*, 1101–1110. [[CrossRef](#)]
48. Archbold, C.T.; Andrews, J.L.; Mandle, R.J.; Cowling, S.J.; Goodby, J.W. Effect of the linking unit on the twist-bend nematic phase in liquid crystal dimers: A comparative study of two homologous series of methylene- and ether-linked dimers. *Liq. Cryst.* **2017**, *44*, 84–92. [[CrossRef](#)]
49. Mandle, R.J.; Voll, C.C.A.; Lewis, D.J.; Goodby, J.W. Etheric bimesogens and the twist-bend nematic phase. *Liq. Cryst.* **2016**, *43*, 13–21. [[CrossRef](#)]
50. Forsyth, E.; Paterson, D.A.; Cruickshank, E.; Strachan, G.J.; Gorecka, E.; Walker, R.; Storey, J.M.D.; Imrie, C.T. Liquid crystal dimers and the twist-bend nematic phase: On the role of spacers and terminal alkyl chains. *J. Mol. Liq.* **2020**, *320*, 114391. [[CrossRef](#)]
51. Stevenson, W.D.; Zou, H.X.; Zeng, X.B.; Welch, C.; Ungar, G.; Mehl, G.H. Dynamic calorimetry and XRD studies of the nematic and twist-bend nematic phase transitions in a series of dimers with increasing spacer length. *Phys. Chem. Chem. Phys.* **2018**, *20*, 25268–25274. [[CrossRef](#)] [[PubMed](#)]
52. Merkel, K.; Loska, B.; Welch, C.; Mehl, G.H.; Kocot, A. Molecular biaxiality determines the helical structure—Infrared measurements of the molecular order in the nematic twist-bend phase of difluoro terphenyl dimer. *Phys. Chem. Chem. Phys.* **2021**, *23*, 4151–4160. [[CrossRef](#)] [[PubMed](#)]
53. Arakawa, Y.; Komatsu, K.; Shiba, T.; Tsuji, H. Methylene- and thioether-linked cyanobiphenyl-based liquid crystal dimers CBnSCB exhibiting room temperature twist-bend nematic phases and glasses. *Mater. Adv.* **2021**, *2*, 1760–1773. [[CrossRef](#)]
54. Paterson, D.A.; Walker, R.; Abberley, J.P.; Forestier, J.; Harrison, W.T.A.; Storey, J.M.D.; Pocięcha, D.; Gorecka, E.; Imrie, C.T. Azobenzene-based liquid crystal dimers and the twist-bend nematic phase. *Liq. Cryst.* **2017**, *44*, 2060–2078. [[CrossRef](#)]
55. Walker, R.; Majewska, M.; Pocięcha, D.; Makal, A.; Storey, J.M.D.; Gorecka, E.; Imrie, C.T. Twist-Bend Nematic Glasses: The Synthesis and Characterisation of Pyrene-based Nonsymmetric Dimers. *Chemphyschem* **2021**, *22*, 461–470. [[CrossRef](#)] [[PubMed](#)]
56. Strachan, G.J.; Harrison, W.T.A.; Storey, J.M.D.; Imrie, C.T. Understanding the remarkable difference in liquid crystal behaviour between secondary and tertiary amides: The synthesis and characterisation of new benzamide-based liquid crystal dimers. *Phys. Chem. Chem. Phys.* **2021**, *23*, 12600–12611. [[CrossRef](#)]
57. Abberley, J.P.; Storey, J.M.D.; Imrie, C.T. Structure-property relationships in azobenzene-based twist-bend nematogens. *Liq. Cryst.* **2019**, *46*, 2102–2114. [[CrossRef](#)]
58. Sebastian, N.; Tamba, M.G.; Stannarius, R.; de la Fuente, M.R.; Salamonczyk, M.; Cukrov, G.; Gleeson, J.; Sprunt, S.; Jakli, A.; Welch, C.; et al. Mesophase structure and behaviour in bulk and restricted geometry of a dimeric compound exhibiting a nematic-nematic transition. *Phys. Chem. Chem. Phys.* **2016**, *18*, 19299–19308. [[CrossRef](#)]
59. Ahmed, Z.; Welch, C.; Mehl, G.H. The design and investigation of the self-assembly of dimers with two nematic phases. *RSC Adv.* **2015**, *5*, 93513–93521. [[CrossRef](#)]
60. Arakawa, Y.; Ishida, Y.; Tsuji, H. Ether- and Thioether-Linked Naphthalene-Based Liquid-Crystal Dimers: Influence of Chalcogen Linkage and Mesogenic-Arm Symmetry on the Incidence and Stability of the Twist-Bend Nematic Phase. *Chem. Eur. J.* **2020**, *26*, 3767–3775. [[CrossRef](#)]
61. Arakawa, Y.; Komatsu, K.; Ishida, Y.; Tsuji, H. Thioether-linked azobenzene-based liquid crystal dimers exhibiting the twist-bend nematic phase over a wide temperature range. *Liq. Cryst.* **2021**, *48*, 641–652. [[CrossRef](#)]
62. Knezevic, A.; Dokli, I.; Novak, J.; Kontrec, D.; Lesac, A. Fluorinated twist-bend nematogens: The role of intermolecular interaction. *Liq. Cryst.* **2021**, *48*, 756–766. [[CrossRef](#)]
63. Al-Janabi, A.; Mandle, R.J. Utilising Saturated Hydrocarbon Isosteres of para Benzene in the Design of Twist-Bend Nematic Liquid Crystals. *Chemphyschem* **2020**, *21*, 697–701. [[CrossRef](#)] [[PubMed](#)]
64. Mandle, R.J.; Goodby, J.W. Does Topology Dictate the Incidence of the Twist-Bend Phase? Insights Gained from Novel Unsymmetrical Bimesogens. *Chem. Eur. J.* **2016**, *22*, 18456–18464. [[CrossRef](#)]

65. Abberley, J.P.; Jansze, S.M.; Walker, R.; Paterson, D.A.; Henderson, P.A.; Marcelis, A.T.M.; Storey, J.M.D.; Imrie, C.T. Structure-property relationships in twist-bend nematogens: The influence of terminal groups. *Liq. Cryst.* **2017**, *44*, 68–83. [[CrossRef](#)]
66. Ivsic, T.; Baumeister, U.; Dokli, I.; Mikleusevic, A.; Lesac, A. Sensitivity of the N-TB phase formation to the molecular structure of imino-linked dimers. *Liq. Cryst.* **2017**, *44*, 93–105.
67. Mandle, R.J.; Davis, E.J.; Archbold, C.T.; Voll, C.C.A.; Andrews, J.L.; Cowling, S.J.; Goodby, J.W. Apolar Bimesogens and the Incidence of the Twist-Bend Nematic Phase. *Chem. Eur. J.* **2015**, *21*, 8158–8167. [[CrossRef](#)]
68. Mandle, R.J.; Goodby, J.W. Dependence of Mesomorphic Behaviour of Methylene-Linked Dimers and the Stability of the N-TB/N-X Phase upon Choice of Mesogenic Units and Terminal Chain Length. *Chem. Eur. J.* **2016**, *22*, 9366–9374. [[CrossRef](#)]
69. Mandle, R.J.; Goodby, J.W. A Liquid Crystalline Oligomer Exhibiting Nematic and Twist-Bend Nematic Mesophases. *Chemphyschem* **2016**, *17*, 967–970. [[CrossRef](#)]
70. Arakawa, Y.; Komatsu, K.; Inui, S.; Tsuji, H. Thioether-linked liquid crystal dimers and trimers: The twist-bend nematic phase. *J. Mol. Struct.* **2020**, *1199*, 126913. [[CrossRef](#)]
71. Mandle, R.J.; Goodby, J.W. A Nanohelicoidal Nematic Liquid Crystal Formed by a Non-Linear Duplexed Hexamer. *Angew Chem. Int. Ed.* **2018**, *57*, 7096–7100. [[CrossRef](#)] [[PubMed](#)]
72. Tuchband, M.R.; Paterson, D.A.; Salamonczyk, M.; Norman, V.A.; Scarbrough, A.N.; Forsyth, E.; Garcia, E.; Wang, C.; Storey, J.M.D.; Walba, D.M.; et al. Distinct differences in the nanoscale behaviors of the twist-bend liquid crystal phase of a flexible linear trimer and homologous dimer. *Proc. Nat. Acad. Sci. USA* **2019**, *116*, 10698–10704. [[CrossRef](#)] [[PubMed](#)]
73. Arakawa, Y.; Komatsu, K.; Shiba, T.; Tsuji, H. Phase behaviors of classic liquid crystal dimers and trimers: Alternate induction of smectic and twist-bend nematic phases depending on spacer parity for liquid crystal trimers. *J. Mol. Liq.* **2021**, *326*, 115319. [[CrossRef](#)]
74. Majewska, M.M.; Forsyth, E.; Pocięcha, D.; Wang, C.; Storey, J.M.D.; Imrie, C.T.; Gorecka, E. Controlling spontaneous chirality in achiral materials: Liquid crystal oligomers and the heliconical twist-bend nematic phase. *Chem. Commun.* **2022**, *58*, 5285–5288. [[CrossRef](#)] [[PubMed](#)]
75. Jansze, S.M.; Martinez-Felipe, A.; Storey, J.M.D.; Marcelis, A.T.M.; Imrie, C.T. A Twist-Bend Nematic Phase Driven by Hydrogen Bonding. *Angew Chem. Int. Ed.* **2015**, *54*, 643–646. [[CrossRef](#)]
76. Walker, R.; Pocięcha, D.; Abberley, J.P.; Martinez-Felipe, A.; Paterson, D.A.; Forsyth, E.; Lawrence, G.B.; Henderson, P.A.; Storey, J.M.D.; Gorecka, E.; et al. Spontaneous chirality through mixing achiral components: A twist-bend nematic phase driven by hydrogen-bonding between unlike components. *Chem. Commun.* **2018**, *54*, 3383–3386. [[CrossRef](#)]
77. Walker, R.; Pocięcha, D.; Martinez-Felipe, A.; Storey, J.M.D.; Gorecka, E.; Imrie, C.T. Twist-Bend Nematogenic Supramolecular Dimers and Trimers Formed by Hydrogen Bonding. *Crystals* **2020**, *10*, 175. [[CrossRef](#)]
78. Walker, R.; Pocięcha, D.; Crawford, C.A.; Storey, J.M.D.; Gorecka, E.; Imrie, C.T. Hydrogen bonding and the design of twist-bend nematogens. *J. Mol. Liq.* **2020**, *303*, 112630. [[CrossRef](#)]
79. Walker, R.; Pocięcha, D.; Salamonczyk, M.; Storey, J.M.D.; Gorecka, E.; Imrie, C.T. Supramolecular liquid crystals exhibiting a chiral twist-bend nematic phase. *Mater. Adv.* **2020**, *1*, 1622–1630. [[CrossRef](#)]
80. Chen, D.; Nakata, M.; Shao, R.; Tuchband, M.R.; Shuai, M.; Baumeister, U.; Weissflog, W.; Walba, D.M.; Glaser, M.A.; MacLennan, J.E.; et al. Twist-bend heliconical chiral nematic liquid crystal phase of an achiral rigid bent-core mesogen. *Phys. Rev. E.* **2014**, *89*, 022506. [[CrossRef](#)]
81. Sreenilayam, S.P.; Panov, V.P.; Vij, J.K.; Shanker, G. The N-TB phase in an achiral asymmetrical bent-core liquid crystal terminated with symmetric alkyl chains. *Liq. Cryst.* **2017**, *44*, 244–253.
82. Stevenson, W.D.; An, J.G.; Zeng, X.B.; Xue, M.; Zou, H.X.; Liu, Y.S.; Ungar, G. Twist-bend nematic phase in biphenylethane-based copolyethers. *Soft Matter* **2018**, *14*, 3003–3011. [[CrossRef](#)] [[PubMed](#)]
83. Mandle, R.J. A Ten-Year Perspective on Twist-Bend Nematic Materials. *Molecules* **2022**, *27*, 2689. [[CrossRef](#)] [[PubMed](#)]
84. Greco, C.; Luckhurst, G.R.; Ferrarini, A. Molecular geometry, twist-bend nematic phase and unconventional elasticity: A generalised Maier-Saupe theory. *Soft Matter* **2014**, *10*, 9318–9323. [[CrossRef](#)]
85. Paterson, D.A.; Xiang, J.; Singh, G.; Walker, R.; Agra-Kooijman, D.M.; Martinez-Felipe, A.; Gan, M.; Storey, J.M.D.; Kumar, S.; Lavrentovich, O.D.; et al. Reversible Isothermal Twist-Bend Nematic-Nematic Phase Transition Driven by the Photoisomerization of an Azobenzene-Based Nonsymmetric Liquid Crystal Dimer. *J. Am. Chem. Soc.* **2016**, *138*, 5283–5289. [[CrossRef](#)]
86. Zaton, D.; Karamoula, A.; Strachan, G.J.; Storey, J.M.D.; Imrie, C.T.; Martinez-Felipe, A. Photo-driven effects in twist-bend nematic phases: Dynamic and memory response of liquid crystalline dimers. *J. Mol. Liq.* **2021**, *344*, 117680. [[CrossRef](#)]
87. Aya, S.; Salamon, P.; Paterson, D.A.; Storey, J.M.D.; Imrie, C.T.; Araoka, F.; Jakli, A.; Buka, A. Fast-and-Giant Photorheological Effect in a Liquid Crystal Dimer. *Adv. Mater. Interfaces* **2019**, *6*, 1802032. [[CrossRef](#)]
88. Dawood, A.A.; Gossel, M.C.; Luckhurst, G.R.; Richardson, R.M.; Timimi, B.A.; Wells, N.J.; Yousif, Y.Z. Twist-bend nematics, liquid crystal dimers, structure-property relations. *Liq. Cryst.* **2017**, *44*, 106–126.
89. Mandle, R.J.; Goodby, J.W. Intercalated soft-crystalline mesophase exhibited by an unsymmetrical twist-bend nematogen. *Crystengcomm* **2016**, *18*, 8794–8802. [[CrossRef](#)]
90. Mandle, R.J.; Goodby, J.W. A twist-bend nematic to an intercalated, anticlinic, biaxial phase transition in liquid crystal bimesogens. *Soft Matter* **2016**, *12*, 1436–1443. [[CrossRef](#)]
91. Pocięcha, D.; Vaupotic, N.; Majewska, M.; Cruickshank, E.; Walker, R.; Storey, J.M.D.; Imrie, C.T.; Wang, C.; Gorecka, E. Photonic Bandgap in Achiral Liquid Crystals—A Twist on a Twist. *Adv. Mater.* **2021**, *33*, 2103288. [[CrossRef](#)] [[PubMed](#)]

92. Link, D.R.; Natale, G.; Shao, R.; MacLennan, J.E.; Clark, N.A.; Korblova, E.; Walba, D.M. Spontaneous formation of macroscopic chiral domains in a fluid smectic phase of achiral molecules. *Science* **1997**, *278*, 1924–1927. [[CrossRef](#)] [[PubMed](#)]
93. Matraszek, J.; Topnani, N.; Vaupotic, N.; Takezoe, H.; Mieczkowski, J.; Pocięcha, D.; Gorecka, E. Monolayer Filaments versus Multilayer Stacking of Bent-Core Molecules. *Angew Chem. Int. Ed.* **2016**, *55*, 3468–3472. [[CrossRef](#)] [[PubMed](#)]
94. Salamonczyk, M.; Vaupotic, N.; Pocięcha, D.; Walker, R.; Storey, J.M.D.; Imrie, C.T.; Wang, C.; Zhu, C.H.; Gorecka, E. Multi-level chirality in liquid crystals formed by achiral molecules. *Nat. Commun.* **2019**, *10*, 1922. [[CrossRef](#)] [[PubMed](#)]
95. Salili, S.M.; Almeida, R.R.R.; Challa, P.K.; Sprunt, S.N.; Gleeson, J.T.; Jaklia, A. Spontaneously modulated chiral nematic structures of flexible bent-core liquid crystal dimers. *Liq. Cryst.* **2017**, *44*, 160–167. [[CrossRef](#)]
96. Takezoe, H.; Gorecka, E.; Cepic, M. Antiferroelectric liquid crystals: Interplay of simplicity and complexity. *Rev. Mod. Phys.* **2010**, *82*, 897–937. [[CrossRef](#)]
97. Mach, P.; Pindak, R.; Levelut, A.M.; Barois, P.; Nguyen, H.T.; Huang, C.C.; Furenlid, L. Structural characterization of various chiral smectic-C phases by resonant X-ray scattering. *Phys. Rev. Lett.* **1998**, *81*, 1015–1018. [[CrossRef](#)]
98. Tschierske, C. The Magic 4-Cyanoresorcinols-Their Role in the Understanding of Phenomena at the Rod-Banana Cross-Over and Relations to Twist-Bend Phases and Other Newly Emerging LC Phase Types. *Liq. Cryst.* **2022**, *49*, 1043–1077. [[CrossRef](#)]
99. Sreenilayam, S.P.; Panarin, Y.P.; Vij, J.K.; Panov, V.P.; Lehmann, A.; Poppe, M.; Prehm, M.; Tschierske, C. Spontaneous helix formation in non-chiral bent-core liquid crystals with fast linear electro-optic effect. *Nat. Commun.* **2016**, *7*, 11369. [[CrossRef](#)]
100. Sreenilayam, S.P.; Panarin, Y.P.; Vij, J.K.; Lehmann, A.; Poppe, M.; Tschierske, C. Development of ferroelectricity in the smectic phases of 4-cyanoresorcinol derived achiral bent-core liquid crystals with long terminal alkyl chains. *Phys. Rev. Mater.* **2017**, *1*, 035604. [[CrossRef](#)]
101. Sekine, T.; Niori, T.; Watanabe, J.; Furukawa, T.; Choi, S.W.; Takezoe, H. Spontaneous helix formation in smectic liquid crystals comprising achiral molecules. *J. Mater. Chem.* **1997**, *7*, 1307–1309. [[CrossRef](#)]
102. Cady, A.; Pitney, J.A.; Pindak, R.; Matkin, L.S.; Watson, S.J.; Gleeson, H.F.; Cluzeau, P.; Barois, P.; Levelut, A.M.; Caliebe, W.; et al. Orientational ordering in the chiral smectic-C-F12\* liquid crystal phase determined by resonant polarized x-ray diffraction. *Phys. Rev. E* **2001**, *64*, 050702. [[CrossRef](#)] [[PubMed](#)]
103. Cruickshank, E.; Anderson, K.; Storey, J.M.D.; Imrie, C.T.; Gorecka, E.; Pocięcha, D.; Makal, A.; Majewska, M.M. Helical phases assembled from achiral molecules: Twist-bend nematic and helical filamentary B-4 phases formed by mesogenic dimers. *J. Mol. Liq.* **2022**, *346*, 118180. [[CrossRef](#)]
104. Alshammari, A.F.; Pocięcha, D.; Walker, R.; Storey, J.M.D.; Gorecka, E.; Imrie, C.T. New patterns of twist-bend liquid crystal phase behaviour: The synthesis and characterisation of the 1-(4-cyanobiphenyl-4'-yl)-10-(4-alkylaniline-benzylidene-4'-oxy)decanes (CB10O.m). *Soft Matter*. **2022**, *18*, 4679–4688. [[CrossRef](#)]